AD-A161 862 THEORY OF THE CURRENT-DRIVEN ION CYCLOTRON INSTABILITY IN THE BOTTOMSIDE IONOSPHERE(U) NAVAL RESEARCH LAB WASHINGTON DC P SATYANARAYANA ET AL. 11 NOV 85 1/1

UNCLASSIFIED NRL-MR-5656 F/G 4/1 NL

END
FILMED
DTIC

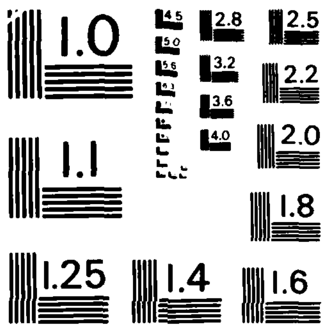

MICROCOPY RESOLUTION TEST CHART
NATIONAL BUREAU OF STANDARDS-1963-A

(2)

NRL Memorandum Report 5656

Theory of the Current-Driven Ion Cyclotron Instability in the Bottomside Ionosphere

P. SATYANARAYANA AND P. K. CHATURVEDI

Science Applications International Corporation
McLean, VA 22102

M. J. KESKINEN AND J. D. HUBA

Geophysical and Plasma Dynamics Branch
Plasma Physics Division

S. L. OSSAKOW

Plasma Physics Division

November 11, 1985

This research was supported by the Defense Nuclear Agency under Subtask QIEQMXBB, work unit 00005 and work unit title "Plasma Structure Evolution," also by the National Aeronautics and Space Administration and the Office of Naval Research.

NAVAL RESEARCH LABORATORY
Washington, D.C.

AD-A161 862

SECURITY CLASSIFICATION OF THIS PAGE

REPORT DOCUMENTATION PAGE

1a REPORT SECURITY CLASSIFICATION: UNCLASSIFIED		1b RESTRICTIVE MARKINGS	
2a SECURITY CLASSIFICATION AUTHORITY		3 DISTRIBUTION/AVAILABILITY OF REPORT: Approved for public release; distribution unlimited.	
2b DECLASSIFICATION/DOWNGRADING SCHEDULE			
4 PERFORMING ORGANIZATION REPORT NUMBER(S): NRL Memorandum Report 5656		5 MONITORING ORGANIZATION REPORT NUMBER(S)	
6a NAME OF PERFORMING ORGANIZATION: Naval Research Laboratory	6b OFFICE SYMBOL (If applicable): Code 4780	7a NAME OF MONITORING ORGANIZATION	
6c ADDRESS (City, State, and ZIP Code): Washington, DC 20375-5000		7b ADDRESS (City, State, and ZIP Code)	
8a NAME OF FUNDING/SPONSORING ORGANIZATION: DNA, NASA and ONR	8b OFFICE SYMBOL (If applicable)	9 PROCUREMENT INSTRUMENT IDENTIFICATION NUMBER	
8c ADDRESS (City, State, and ZIP Code): Washington, DC 20305 Washington, DC 20546 Arlington, VA 22217		10 SOURCE OF FUNDING NUMBERS	

PROGRAM ELEMENT NO	PROJECT NO	TASK NO	WORK UNIT ACCESSION NO
(See page ii)			

11 TITLE (Include Security Classification)

Theory of the Current-Driven Ion Cyclotron Instability in the Bottomside Ionosphere

12 PERSONAL AUTHOR(S)

Satyanarayana, P.,* Chaturvedi, P.K.,* Keskinen, M.J., Huba, J.D. and Ossakow, S.L.

13a TYPE OF REPORT	13b TIME COVERED	14 DATE OF REPORT (Year, Month, Day)	15 PAGE COUNT
Interim	FROM ____ TO ____	1985 November 11	49

16 SUPPLEMENTARY NOTATION

*Science Applications International Corporation, McLean, VA 22102 (Continues)

17 COSATI CODES			18 SUBJECT TERMS (Continue on reverse if necessary and identify by block number)
FIELD	GROUP	SUB-GROUP	Currents; High latitude ionosphere; Collisions; Ion-cyclotron instability; Nonlinear theory

19 ABSTRACT (Continue on reverse if necessary and identify by block number)

A theory of the current-driven electrostatic ion cyclotron (EIC) instability in the collisional bottomside ionosphere is presented. It is found that the electron collisions are destabilizing and are crucial for the excitation of the EIC instability in the collisional bottomside ionosphere. Furthermore, the growth rates of the ion cyclotron instability in the bottomside ionosphere maximize for $k_\perp \rho_i \geqslant 1$ where $2\pi/k_\perp$ is the mode scale size perpendicular to the magnetic field and ρ_i the ion gyroradius. Realistic plasma density and temperature profiles typical of the high latitude ionosphere are used to compute the altitude dependence of the linear growth rate of the maximally growing modes and critical drift velocity of the EIC instability. The maximally growing modes correspond to observed meter size irregularities and the threshold drift velocity required for the excitation of EIC instability is lower for heavier (NO^+, O^+) ions than that for the lighter (H^+) ions. Dupree's resonance broadening theory is used to estimate nonlinear saturated amplitudes for the ion cyclotron instability in the high latitude ionosphere. Comparison with

(Continues)

20 DISTRIBUTION/AVAILABILITY OF ABSTRACT	21 ABSTRACT SECURITY CLASSIFICATION
☒ UNCLASSIFIED/UNLIMITED ☐ SAME AS RPT ☐ DTIC USERS	UNCLASSIFIED

22a NAME OF RESPONSIBLE INDIVIDUAL	22b TELEPHONE (Include Area Code)	22c OFFICE SYMBOL
J. D. Huba	(202) 767-3630	Code 4780

DD FORM 1473, 84 MAR 83 APR edition may be used until exhausted. All other editions are obsolete

SECURITY CLASSIFICATION OF THIS PAGE

10. SOURCE OF FUNDING NUMBERS

PROGRAM ELEMENT NO.	PROJECT NO.	TASK NO.	WORK UNIT ACCESSION NO.
62715H 61153N	RR033-02-44	S-14534-D	DN580-072

16. SUPPLEMENTARY NOTATION (Continued)

This research was supported by the Defense Nuclear Agency under Subtask QIEQMXBB, work unit 00005 and work unit title "Plasma Structure Evolution," also by the National Aeronautics and Space Administration and the Office of Naval Research.

19. ABSTRACT (Continued)

experimental observations is also made. It is conjectured that the EIC instability in the bottomside ionosphere could be a source of transversely accelerated heavier ions and energetic heavy ion conic distributions at higher altitudes.

CONTENTS

THEORY OF THE CURRENT-DRIVEN ION CYCLOTRON INSTABILITY IN THE BOTTOMSIDE IONOSPHERE

1. Introduction

Electrostatic ion cyclotron (EIC) waves are one of the more important plasma wave modes in the near earth space plasma environment. Recently, EIC waves have been invoked to explain, among other effects, strong perpendicular ion heating leading to the formation of ion conics [Okuda and Ashour-Abdalla, 1981]. Ion cyclotron wave phenomena have been observed both at high (several R_e) and low (< 1000 km) altitudes along auroral field lines. Kintner et al. [1978, 1979] have reported H^+ EIC wave observations using S3-3 satellite data at high altitudes in the auroral zone. At low altitudes, O^+ EIC waves have been observed [Ogawa et al., 1981] on a sounding rocket equatorward of a discrete auroral arc. Yau et al. [1983], also using sounding rocket data, have reported particle and wave observations of low altitude (400-600 km) ionospheric ion acceleration events consistent with ion cyclotron wave phenomena. Bering [1984] has given indirect, but compelling, evidence of short wavelength ($k_\perp \rho_i \gtrsim 1$ where $2\pi/k_\perp$ is the density fluctuation scale size perpendicular to the magnetic field and ρ_i is the ion gyroradius) ion cyclotron wave activity at low altitudes (< 350 km) in the diffuse aurora using sounding rocket data. Evidence for short wavelength ($k_\perp \rho_i \gtrsim 1$) ion cyclotron wave emissions in the auroral E-region has been presented by Fejer et al. [1984] using backscatter radar observations. Photometric observations in the bright auroras at ~ 130 km altitude by Martelli et al. (1971) indicated excitation of EIC waves at frequencies lying between 25 and 32 Hz, correspoding to gyrofrequencies of NO^+ and O_2^+. Bythrow et al. (1984), using Hilat satellite data, have concluded that the very large earthward directed currents seen near the equatorward edge of the diffuse aurora exceed the threshold for the excitation of ion cyclotron waves.

Kindel and Kennel [1971] first discussed the ion cyclotron instability in a space plasma context by showing that the electrostatic ion cyclotron instability has the lowest threshold among various current-driven instabilities in the high latitude auroral space plasma. They only briefly discussed the role of weak collisional effects on the evolution of the EIC wave instability. They did note, however, in the context of the EIC

Manuscript approved July 9, 1985.

instability that electron collisions were destabilizing and ion collisions were stabilizing. Physically, the ion cyclotron instability is related to the dissipative effect on electrons in their parallel motion which impedes the "instantaneous" redistribution of the electron fluid to a Boltzman-like distribution in the wave potential. In the collisionless limit, the dissipation is due to the wave-particle (Landau) resonance, while in the collisional case, it is caused by the electron collisions with ions (or neutrals). The results of Kindel and Kennel [1971] are only applicable to the collisionless and weakly-collisional topside ionosphere [Chaturvedi et al., 1984]. Recently Ganguli et al. (1985) have proposed a mechanism that depends on the inhomogeneity of the transverse electric fields to generate ion cyclotron waves in a collisionless plasma in the absence of field-aligned currents. However, several of the aforementioned experimental studies have indicated ion cyclotron wave emissions can occur at low altitudes in the collisional bottomside ionosphere. D'Angelo [1973], using the work of Varma and Bhadra [1964] and Levine and Kuckes [1966], has shown that the current-driven EIC instability might be excited at low altitudes (E-region) where the ion-neutral collision frequency is comparable to the ion cyclotron frequency. This work has been extended to the collisional auroral F-region altitudes by Chaturvedi [1976] based on the analyses of Chaturvedi and Kaw [1975] and Milić [1972]. However, Chaturvedi [1976] considers collisional effects on the ion cyclotron instability using a fluid approximation $(k_\perp \rho_i < 1)$. This analysis is not applicable to the recent experimental observations which indicate $k_\perp \rho_i \gtrsim 1$. For example, Bering(1984) and Fejer et al. (1984) have reported observations of meter size irregularities corresponding to $k_\perp \rho_i \approx 1$. Indeed, the transition between collisionless and collisional excitation of the ion cyclotron instability, the approximate altitude of this transition, and the dependence of growth rate of the ion cyclotron instability on ambient high latitude ionospheric plasma parameters is not well-defined.

In addition to observations indicating existence of EIC waves in the bottomside ionosphere, the presence of energetic heavy ions at 1400 km altitude was first documented by Hoffman et al. [1974]. Energy and pitch angle distributions of various ion species obtained by S3-3 and PROGNOZ-7 satellite measurements provide evidence for the presence of energetic heavier ion species (NO^+ and O^+, for example) at altitudes of a few

thousand kilometers or more (Hultqvist, 1983; Yau et al., 1984). The pitch angle distributions of ions ranged from being field-aligned (ion beams) to conical, in which case the flux peaks at an angle to the geomagnetic field. The pitch angle distributions measured at energies less than 650 eV are relatively field-aligned, while those at 1 keV and above have a conical distribution with no field-aligned component [Klumpar et al., 1984]. Recent data from DE-1 also showed that the high altitude Polar Cap region contains upflowing heavy molecular ions such as NO^+, O_2^+ and N_2^+ (Craven et al., 1985). These data suggest that the source for these energetic heavy ions might be located in the ionosphere (Hultqvist, 1983). Based on our linear theoretical analysis, we conjecture that the current driven EIC waves at the ion (heavy) cyclotron frequency could selectively accelerate the heavier ions, such as NO^+, O_2^+ and O^+, in the transverse direction. Thus the bottomside ionosphere can act as a source for the heavier ion conics observed at magnetospheric altitudes.

In this paper we study the EIC instability in the bottomside collisional ionosphere. We find that the growth rates of the EIC instability in the bottomside ionosphere maximize for $k_\perp \rho_i \approx 1$. In Sec. 2, we present the general dispersion relation for EIC waves in a collisional plasma which we solve analytically both in the collisionless, weakly collisional, and strongly collisional limits. We also solve the full dispersion relation numerically, using the plasma density and temparature profiles obtained from the Sondrestrom radar (Kelly, 1983). The dispersion relation is solved for the maximally growing modes, for which $k_\perp \rho_i \approx 1.4$, corresponding to observed meter size irregularities. In Sec. 3, we compute expected nonlinear saturation amplitudes of the electrostatic ion cyclotron instability in a collisional plasma based upon Dupree's resonance broadening theory and compare with experimental observations. Finally in Sec. 4, we summarize and discuss our results.

2. Linear Theory

We consider a homogeneous plasma in a uniform magnetic field along the z-direction, $\underline{B} = B\hat{z}$. The plasma is collisional and the main source of free energy is due to the magnetic field aligned currents. In this paper we ignore inhomogeneous effects, e.g., density and temperature gradients and, as a result, use local theory. Furthermore, we assume the scale height in

the high latitude ionosphere to be much larger than the parallel wavelengths involved. In our attempt to understand ion cyclotron instabilities in the bottomside ionosphere, we include collisional effects and use the general dispersion relation derived by Clemmow and Dougherty (1969). In order to include collisional effects we use a number conserving BGK collision model. This model can also be shown to conserve momentum if the electrons are assumed to carry the bulk of the current and the ions are considered to be at rest. Under these conditions, the BGK model reproduces well electron-neutral (ν_{en}), electron-ion (ν_{ei}), and ion-neutral (ν_{in}) collisions. However, the BGK model does not reproduce well ion-ion (ν_{ii}) or electron-electron collisions and a different collision model, e.g., Fokker-Planck approximiation, must be used. Since we will be considering bottomside F-region altitudes ($z \lesssim$ 300-400 km), $\nu_{ii} \lesssim \nu_{in}$ is satisfied. Electron viscous effects (ν_{ee}) are negligible because the electron Larmor radius is much smaller than the perpendicular wavelengths of interest. In section 2.2, we do include a phenomenological model for ν_{ii} in our numerical computation of growth rates and marginal stability criteria for the electrostatic ion cyclotron instability.

We utilize the dispersion relation derived by Clemmow and Dougherty (1969). We list only the salient features of the derivation here. The equilibrium function is a drifting Maxwellian

$$f_{oj} = N_{oj} \left(\frac{m_j}{2\pi T_j}\right)^{3/2} \exp[-(V_\perp^{\,2} + (V_\parallel - V_{dj})^2)/V_j^{\,2}] \qquad (1)$$

where N_{oj}, m_j, T_j, V_{dj} and V_j are the density, mass, temperature, drift and thermal velocities of the j^{th} species, respectively. The perturbed distribution function (where $f_j = f_{oj} + f_{1j}$) is given as, using a BGK collision model,

$$\frac{\partial f_1}{\partial t} + \underline{V}\cdot\frac{\partial f_1}{\partial \underline{x}} + \frac{e}{mc}(\underline{V} \times \underline{B}) \cdot \frac{\partial f_1}{\partial \underline{V}} = \sum_j \nu_j [f_{1j} - (N_{1j}/N_{oj}) f_{oj}] \qquad (2)$$

where

$$N_{1j} = \frac{-(e/m)\nabla\phi_1 \int D^{-1}\partial f_o/\partial V \, d^3V}{1 - (\nu_j/N_o)\int D^{-1} f_o d^3V} \quad \text{and } D \equiv i(\omega - i\nu_j - \underline{k}\cdot\underline{V})$$

For a low β ($8\pi nkT/B^2 << 1$) plasma and perturbations of the form $f_1 \propto \exp[-i(\omega t - \underline{k}\cdot\underline{x})]$ the dispersion relation is given as [Kindel and Kennel, 1971]

$$-k_{\perp}^2 = \sum_j \frac{\sum_{n=-\infty}^{\infty} \left(\frac{\Gamma_n(b_j)}{\lambda_{dj}^2}\right)\left[1 + \frac{\tilde{\omega}_j}{k_{\parallel} V_j} Z(\xi_j)\right]}{1 + \left(\frac{i\nu_j}{k_{\parallel} V_j}\right) \sum_{n=-\infty}^{\infty} \Gamma_n(b_j) Z(\xi_j)} \tag{3}$$

where

$$b_j = k_{\perp}^2 \rho_j^2 /2$$

$$\rho_j = V_j/\Omega_j$$

$$\Omega_j = q_j B/m_j c$$

$$\lambda_{dj} = (T_j/4\pi n_j q_j^2)^{1/2}$$

$$V_j = 2T_j/m_j$$

$$\tilde{\omega}_j = \omega - k_{\parallel} V_{dj} + i\nu_j$$

$$\xi_j = \frac{\tilde{\omega} + n\Omega_j}{k_{\parallel} V_j}$$

$$\Gamma_n = I_n(b_j)e^{-b_j}$$

where $I_n(b)$ is the modifed Bessel function of n^{th} order and $Z(\xi)$ is the plasma dispersion function, and $\nu_j = \nu_{jn}$ is the collision frequency of the j^{th} species with neutrals and q_j is the charge of the species ($\pm$ e). In the case of electrons, Coulomb collisons can also be included and we define $\nu_e = \nu_{ei} + \nu_{en}$.

The effects of collisions are reflected in the shifted frequency $\tilde{\omega}$ (by $i\nu_j$) and more importantly in the additional term proportional to $\nu_j/k_\parallel V_j$ in the denominator of Eq. (3). In fact, this term gives rise to instability in the collisional domain. This local dispersion relation is assumed to describe both the collisional bottomside and collisionless topside ionosphere. We assume quasi-neutrality and solve equation (3) analytically in the collisionless, weakly collisional, and strongly collisional (fluid) limits.

2.1 Collisionless Domain

By setting $\nu_j = 0$ in equation (3) we immediately recover the collisionless dispersion relation (Drummond and Rosenbluth, 1962; Kindel and Kennel, 1971). Furthermore if we set $n = 0$ for electrons and $n = 1$ for ions and expand the plasma dispersion function $Z(\xi)$ such that the electrons are treated kinetically and the ions are treated in the fluid limit ($\xi_e << 1$ and $\xi_i >> 1$, respectively) we obtain their results:

$$\omega_r/\Omega_i = 1 + \tau \, \Gamma_1(b_i) \tag{4}$$

$$\gamma/\Omega_i = -\tau \, (\pi/2)^{1/2} \, \Gamma_1(b_i) \, \frac{(\omega_r - k_\parallel V_d)}{k_\parallel V_e} \tag{5}$$

where $\tau = T_e/T_i$ and $V_d = V_{de} - V_{di}$. We note here that, as will be shown in sec. 2.2, the numerical solutions of equation (3) agrees with equations (4) and (5) if $n = 1$ for ions. However, for $n > 1$ a higher growth rate is observed, which saturates for $n = 4$. Consequently, the critical drift velocities given in Kindel and Kennel (1971) are overestimated and the growth rates are underestimated.

2.2 Weakly Collisional Limit

The analysis in this limit was also attempted by Kindel and Kennel (1971). We expand the electron Z-function in the small argument limit, $\xi_e << 1$, and retain only $n = 0$ terms in the electron part of the dispersion relation. The electron contribution to equation (3) is given as

$$D_e = \frac{1}{\tau} \frac{1 + i\sqrt{\pi}\xi_e}{1 - \sqrt{\pi}\frac{\nu_e}{k_\parallel V_e}\xi_e}$$

$$= \frac{1}{\tau}\left[1 + i\sqrt{\pi}\frac{(\omega - k_\parallel V_d)}{k_\parallel V_e(1 - \sqrt{\pi}\ \nu_e/k_\parallel V_e)}\right] \tag{6}$$

Here we have assumed $b_e << 1$ which gives $\Gamma_o(b_e) = 1$. We expand the ion Z-function in the large argument limit, $\xi_i >> 1$. The ion contribution of equation (3) is given as

$$D_i = -\frac{\sum_n \frac{\omega + i\nu_i}{\omega + n\Omega + i\nu_i}\Gamma_n(b_i)}{1 - i\nu_i \sum_n \frac{\Gamma_n(b_i)}{\omega + n\Omega + i\nu_i}} \tag{7}$$

For $\nu_i/\Omega_i < 1$ the ion contribution becomes

$$D_i = -f_n\left[(\omega - \nu_i^2 f_n) + i\nu_i(1 + \omega f_n)\right] \tag{8}$$

where

$$f_n \equiv \sum \frac{\Gamma_n}{\omega + n\Omega + i\nu_i}. \tag{9}$$

For $\nu_i/\omega < 1$ the dispersion relation then becomes $D = D_e + D_i = 0$ or

$$\frac{1}{\tau}\left[1 + i\pi\Gamma\frac{(\omega - k_\parallel V_d)}{k_\parallel V_e(1 - \Gamma_1\nu_e/k_\parallel V_e}\right] = -f_n\ (\omega + i\nu_i + \omega\nu_i f_n) \tag{10}$$

From the real part of equation, we obtain the usual result

$$\omega_r = \Omega_i[1 + \tau\ \Gamma_1(b_i)] \tag{11}$$

and from the imaginary part we obtain

$$\gamma/\omega_r = -2\sqrt{\pi}\ \tau\Gamma_1(b_i)\frac{(\omega_r - k_\parallel V_d)}{k_\parallel V_e}\left(1 + \sqrt{\pi}\frac{\nu_e}{k_\parallel V_e}\right) - \nu_i/\Omega_i\left(1 + \frac{1}{\tau}\right) \tag{12}$$

which leads to the collisionless result of Drummond and Rosenbluth (1962) and Kindel and Kennel (1971) in equation (5) when $\nu_e = \nu_i = 0$. Equation (12) shows that the electron collisions have a destabilizing influence whereas the ion collisions are stabilizing. In the short wavelength limit, $\nu_e/k_\parallel V_e \ll 1$, the ion collisions override the destabilizing influence of electron collisions. However, we show in the next section that the electron collisions dominate the ion collisions in the fluid limit, $\nu_e/k_\parallel V_e \gg 1$.

2.3 Strongly collisional limit

In this limit the electron mean freepath $\lambda_e \ll \lambda_\parallel$ and thus $\nu_e/k_\parallel V_e \gg 1$. For $\nu_e/k_\parallel V_e \gg 1$, we can expand the electron Z-function in the large argument limit while still satisfying $V_i < V_d \lesssim V_e$, obtaining

$$D_e = -\frac{1}{2\tau}\,\frac{\Gamma_o(b_e)}{\xi_e^{\,2} - \dfrac{i\,\nu_e}{k_\parallel^{\,2} V_e^{\,2}}\,\tilde{\omega}\,(1 + 1/2\xi_e^{\,2})\,\Gamma_o(b_e)} \tag{13}$$

The ion contribution is obtained, as before, by expanding the Z-function in the large argument limit, $\xi_i \gg 1$, as

$$D_i = G - \Gamma_1(b_i)\,\frac{\omega}{\omega - \Omega_i} \tag{14}$$

where

$$G = 1 - \frac{1 - \Gamma_0(b_i)}{b_i} \tag{15}$$

Now, the dispersion relation becomes

$$D = D_e + D_i \approx 0$$

from which the growth rate and real frequency can be written as

$$\omega_r/\Omega_i = 1 + \tau\Gamma_1(b_i)\,(1 - \tau G)\,\left(1 - \frac{(\Omega_i - k_\parallel V_d)^2}{k_\parallel^{\,2} V_e^{\,2}}\,\frac{1}{\Gamma_0(b_e) + \alpha}\right) \tag{16}$$

$$\gamma/\omega_r = \frac{-2\tau\Gamma_1(b_i)(1-\tau G)}{(\Gamma_0(b_e)+\alpha)}\frac{(\omega_r - k_\parallel V_d)\nu_e}{k_\parallel^2 v_e^2} \tag{17}$$

where $\alpha = (\nu_e^2/\Omega_e^2)(k_\perp^2/k_\parallel^2)$. For $b_i << 1$ and $\nu_e/\Omega_e << 1$ equations (16) and (17) reduce to that obtained by Chaturvedi (1976) who used a fluid analysis. We see from equations (16) and (17) that the real frequency is not significantly different from the collisionless result (see equation 4) and the growth rate is directly proportional to ν_e and V_d but has a peak in ν_e at $\nu_e = \Omega_e(k_\parallel/k_y)[\Gamma_0(b_e)]^{1/2}$. Since $\nu_e \propto T_e^{-3/2}$ for Coulomb collisions we see from equation (17) that initially the growth rate decreases with T_e as $T_e^{-3/2}$ and for strong collisions the growth rate increases as $T_e^{3/2}$ indicating a minimum as a function of τ (for a fixed T_i). This is in sharp contrast to the collisionless case where the growth rate increases as a function of τ (equation 5).

2.4 Marginal stability analysis

In the collisionless domain several authors have estimated the drift velocity thresholds for the onset of the ion cyclotron instability (see for example, Drummond and Rosenbluth, 1962; Kindel and Kennel, 1971). Kindel and Kennel (1971) have examined briefly the effects of ion-neutral collisions and weak electron-neutral collisions. Their expression for threshold drift velocity shows that while the electron-neutral collisions could destabilize the EIC instability, the ion-neutral collisions strongly stabilize the EIC instability.

In the weakly collisional limit $\nu_e/k_\parallel v_e << 1$, we expand the electron Z-function in the small argument limit. The electron part of the dispersion relation in the above limit together with the ion part in the large argument limit yield the dispersion relation given in equation (10). The imaginary part of equation (10) yields, for $\gamma = 0$,

$$\omega_r - k_\parallel V_c = \frac{\tau}{\sqrt{\pi}}\left(k_\parallel v_e - \sqrt{\pi}\,\nu_e\right)\frac{f_n \nu_i(1+\omega_r f_n)}{(1-\nu_i^2 f_n^2)} \tag{18}$$

Where V_c is the threshold drift velocity. Considering the resonance at the first harmonic we obtain from equation (18)

$$\frac{V_c}{V_e} = \frac{\omega_r}{k_\parallel V_e} + \frac{\tau\Gamma_1}{\sqrt{\pi}}\left(1 - \frac{\nu_e\sqrt{\pi}}{k_\parallel V_e}\right)\left(\frac{\nu_i}{\omega-\Omega}\right)\left(1 + \frac{\omega_r\Gamma_1}{\omega-\Omega}\right) \tag{19}$$

which agrees with that of Kindel and Kennel (1971). Equation (19) shows that in a weakly collisional limit the critical drift velocity is reduced by electron collisions and increased by ion collisions. For a given ion temperature, increasing the electron temperature increases the critical drift velocity; however, electron collisions reduce the influence of ion collisions.

In the strongly collisional limit $\nu_e/k_\parallel V_e >> 1$ and $\nu_e \gtrsim \omega$, the large argument expansion of the electron and ion Z-functions yields the dispersion relation, equation (15), from which

$$\frac{\Gamma_0(b_e) + \alpha}{\left(\Gamma_0(b_e) + \alpha\right) - 2\,(\tilde{\omega}_e)(\omega - k_\parallel V_c)/k_\parallel^2 V_e^2} + \tau\left\{1 + \bar{\Gamma}_1\left[-\frac{\bar{\omega}}{\bar{\omega} - \Omega_i} + i\sqrt{\pi}\,\frac{\bar{\omega}}{k_\parallel V_i}\,e^{-\xi_i^2}\right]\right\} = 0 \tag{20}$$

where $\bar{\Gamma}_1 = \Gamma_1(b_i)\,(1 + \tau G)$ and $\bar{\omega} = \omega + i\nu_{in}$. From the imaginary part of (20), we obtain for $(\omega - k_\parallel V_c)/k_\parallel V_e << 1$

$$\frac{V_c}{V_e} = \frac{\omega_r}{k_\parallel V_e} + \tau\,\bar{\Gamma}_1\,\frac{k_\parallel V_e}{\nu_e}\left[\frac{\nu_i\Omega_i}{(\omega_r - \Omega_i)^2 + \nu_i^2} + \sqrt{\pi}\,\frac{\omega_r}{k_\parallel V_i}\,e^{-|\xi_i|^2}\right] \tag{21}$$

where ω_r is obtained from the real part as

$$\omega_r = \Omega_i\left[1 + \tau\bar{\Gamma}_1/(1 + \tau)\right] \tag{22}$$

Equation (21) shows that in the strongly collisional limit the critical drift velocity has a markedly different behaviour than in the weakly collisional or collisionless limit. Even for $\nu_i = 0$ the electron collisions reduce the critical drift velocity, which is not the case in the weakly collisional limit (equation 19). Furthermore, ion collisions affect the collisional result differently depending on how strong the collision frequency is compared to $(\omega_r - \Omega_i)$, as can be seen from the second term on the right hand side of equation (21). More importantly, the critical drift velocity has a different behaviour as a function of τ, showing a

minimum in some domains, compared to the collisionless case, where it was shown to increase linearly with τ (Drummond and Rosenbluth, 1962).

2.5 Numerical Results Applied to Auroral F-region

The dispersion relation given in equation (3) describes the obliquely propagating ion cyclotron instability and ion acoustic instability as well ($k_\perp = 0$, $\tau > 1$). In this paper, we confine ourselves to the analysis of the ion cyclotron instability. We illustrate the properties of the EIC instability by solving the dispersion relation numerically using parameters typical of the high latitude ionosphere and compare the numerical results with the analytical results in various regimes of collisionality where possible. We find that the growth rate of the collisional ion cyclotron instability maximizes at $k_\perp \rho_i \approx 1$. Furthemore, $k_\perp \rho_i \approx 1$ also corresponds to modes with $\lambda_\perp \approx 11$m ($\rho_i \approx 2.56$m for O^+), which is on the order of typically observed scale size [Fejer et al., 1984; Bering, 1984].

Typical bottomside auroral zone ionospheric electron density and temperature profiles based on Sondreström incoherent scatter radar data (Kelly, 1983; C.L. Rino, private communication) are shown in Fig. 1 and 2 respectively. Curve B is taken from Kelly (1983) the data being simply extrapolated to 600 km. The two electron density profiles (A and C) are expected to bracket both quiet and disturbed conditions with corresponding F-peak densities of roughly 10^4 and 10^6 cm^{-3}, respectively. The electron-neutral (ν_{en}), electron-ion (ν_{ei}), ion-ion (ν_{ii}) and ion neutral (ν_{in}) collisions based upon the data in Fig. 1 and 2 are calculated using standard expressions (Spitzer, 1962; Banks and Kockarts, 1973). Fig. 3 gives the total electron collision frequency ($\nu_e = \nu_{en} + \nu_{ei}$), while Fig. 4 displays the ion collision ($\nu_i = \nu_{in} + \nu_{ii}$) frequency. These collision frequencies are calculated using the electron density profiles of Fig. 1 (Curve 2, Kelly, 1983). Neutral particle density profiles are taken from Banks and Kockarts, (1973) and fall off exponentially with altitude.

In order to illustrate the destabilizing effects of electron neutral and electron ion collisions on the ion cyclotron instability, we solve the dispersion relation Eq. (3) numerically varying $\nu_e = \nu_{en} + \nu_{ei}$ and keeping other parameters fixed. To illustrate the effect of collisionality of the plasma, Fig. 5 shows the growth rate of the electrostatic ion cyclotron instability (Eq. (3)) as a function of altitude for profile B of Fig. 1,

assuming a pure O^+, e^- plasma and taking $k_\parallel/k_\perp = 0.06$, $V_d/V_e = 0.3$. The growth rate shown is based on $b_i = k_\perp^2 \rho_i^2/2 = 1$ which gives maximum growth. Curve 1 represents the collisionless growth rate ($\nu_e = 0 = \nu_i$). The decrease in growth rate is due to the decrease in τ as one goes down in altitude. Curve 2 (where $\nu_e \neq 0$, $\nu_i = 0$), however, displays the strong destabilization in the 100 to 150 km region and mild destabilization around 300 km. Curve 3,(where $\nu_e \neq 0$, $\nu_i \neq 0$), on the other hand, shows the stabilizing influence of ion collisions. The damping influence of ion-ion collisions is phenomenologically represented by $(\nu_{ii} b_i)/(1 + b_i)$, as discussed in the next paragraph. As a comparison we show in curve 4 the collisionless growth with only ion damping included ($\nu_i \neq 0$, $\nu_e = 0$). Curve 3 represents the growth rate for completely realistic ionospheric conditions for which parameters such as plasma density, electron and ion temparatures and neutral density vary with altitude. Curves 3 and 4 clearly establish the importance of the electron collisions, which overcome the ion damping in the region $100 < z < 130$ and significantly enhance the growth rate in the region $150 < z < 300$.

Figure 6 displays the growth rate of the electrostatic ion cyclotron instability including both electron and ion collisions for the three electron density profiles in Fig. 1 and temperatures shown in Fig. 2 assuming an O^+ ion plasma. Although not explicitly calculated in Eq. (3), the ion-ion collisional damping (ν_{ii}) is included in the calculation of the growth rates of Fig. 6 by modeling this damping with the expression $-\nu_{ii} k_\perp^2 \rho_i^2/(1 + k_\perp^2 \rho_i^2)$ (Y.C. Lee, private communication). This expression reduces to the appropriate viscous damping in both the magnetized ($k_\perp \rho_i < 1$) and unmagnetized ($k_\perp \rho_i >> 1$) limits. Since we are concerned with bottomside characteristics of EIC waves ($\nu_{ii} \lesssim \nu_{in}$), the growth rates will not be extremely sensitive to ν_{ii} in any case. The ion-neutral collisions were treated by BGK model with $\nu_{in} \propto n_o T_i^{1/2}$, where n_0 is the neutral density. Finally, for Fig. 6 the following parameters $k_\parallel/k_\perp = 0.06$, $k_\perp \rho_i = \sqrt{2}$, and $V_d/V_e = 0.3$ are used. Curves A, B and C correspond to the profiles given in Fig. 1. It can be seen from curve A that the growth rate maximizes around 400 km and progressively decreases at lower altitudes due to increased damping by ion-neutral and ion-ion collisions and due to a decrease in the electron temperature (τ decreases with decreasing altitude; see Fig. 2). Curve B, representing a typical

ionosphere has smaller growth rate than curve A above 250 km and slightly higher growth rate than curve A below 250 km. Although electron collisions lead to higher growth, the decrease in τ has greater effect on the collisional instability than on the collisionless instability; hence, the decrease in the growth rate above 250 km. The increase in the growth rate at lower altitudes is mainly due to increased electron collisions. Curve C, representative of a disturbed ionosphere, has peak growth at ~ 250 km in the F-region, the decrease in the growth rate at higher altitudes being mainly due to increased ion-ion collisional damping. Eventually the ion damping decreases at higher altitudes where the collisionless theory is valid above which altitude the growth rate increases due to increasing τ.

Figure 7 gives the threshold drift velocities (V_d/V_e) for the EIC instability for the three electron density profiles of Fig. 1 assuming an O^+ ion plasma taking $k_\parallel/k_\perp = 0.06$ and for maximally growing modes with $k_\perp \rho_i = \sqrt{2}$. For profile B, the electrostatic ion cyclotron instability could be destabilized in the bottomside ionosphere ($\lesssim$ 300 km) for current drift velocities on the order of a tenth of electron thermal velocites, $V_d \leq 0.1\ V_e$. Curves A,B and C again are obtained using the density profiles given in Fig. 1. Comparing this figure with Fig. 6, we see that lower drift velocities are needed at larger growth rates. This figure also shows that the collisional EIC instability can also be excited in the E region, although it shows that it is easier to excite EIC in moderately collisional domain (Curve A) than under disturbed conditions (Curve C).

Figure 8 shows the growth rate of the EIC instability including both electron and ion collision for the three electron density profiles in Fig 1 assuming an NO^+ ion plasma. The growth rates of the EIC instability for an NO^+ plasma are similar to (though slightly lower than) the growth rate for the O^+ plasma (Fig. 6). This is consistent with Eqs. (5), (12) and (17) which indicate that the γ/Ω_i is not a strong function of ion mass. Note that the growth rate is normalized to respective gyro frequencies in each case.

Fig. 9 displays the threshold drift velocities (V_c/V_e) for the EIC instability including both electron and ion collisions using the density profiles of Fig. 1 assuming NO^+ ion plasma. Comparing Fig. 9 with Fig. 7 (O^+ plasma) one notes a slight decrease in the threshold drift velocity as

one goes from O^+ to NO^+. This is also consistent with previous studies (Drummond and Rosenbluth, 1962, Kindel and Kennel, 1971) which have shown that increasing the ion mass decreases the threshold current drift velocity at all T_e/T_i to excite the EIC instability. We have also calculated the growth rates and the critical drift velocities for the Hydrogen plasma. We find the growth rates of H^+ EIC waves to be smaller and the critical drift velocities for excitation of H^+ EIC waves to be much higher; for instance, $V_c/V_e = 0.4$ for H^+ EIC wave excitation for the typical parameters used for O^+ calculations, as compared to $V_c/V_e = 0.1$ for O^+ excitation. These critical drift velocities correspond to extremeley large currents and thus we can conclude that the H^+ EIC waves are not likely to be excited in the bottomside ionosphere. For this reason we do not present the detailed results of H^+ EIC wave calculations.

To further emphasize the heavy ion EIC excitation in the F region, we show the threshold currents in the altitude region 100 km to 600 km. We use the density profile (n_e) from Curve A of Fig. 1, T_e from Fig. 2 and (V_c/V_e) from Figs. 7 and 9 to calculate the threshold current $J = n_e e V_c$. Figure 10 shows the threshold currents required to excite O^+ EIC and NO^+ EIC in O^+ and NO^+ plasmas, respectively for $k_\perp \rho_i = \sqrt{2}$ and $k_\parallel/k_\perp = 0.06$. It is clear from Fig. 10 that NO^+ EIC has lower thresholds than O^+ EIC and the altitude region between 150 km and 200 km and the region above 400 km have lower thresholds. The currents shown near 100 km may not be accurate because the theory may not be valid in this region due to demagnetization of the ions ($\nu_{in}/\Omega_i \sim 1$). The critical currents corresponding to curves B of Figs. 1, 7 and 9 (not shown here) are of the order 200 $\mu A/m^2$ - 1000 $\mu A/m^2$. Thus, for typical ionospheres such as those given by curve B, one requires large currents to support O^+ or NO^+ EIC. Although our calculations are applicable to plasma with single ion species, based on the results presented in Figs. 7, 9, and 10 we can draw qualitative conclusions regarding a multispecies plasma, namely that when H^+, O^+, O_2^+ and NO^+ species are present, EIC waves of heavier species are more susceptible to destabilization by parallel currents. Thus we conclude that NO^+ or O_2^+ EIC instability can be excited more easily in the bottomside F region than the H^+ or O^+ EIC instability. This is consistent with the photometric observations of Martelli et al. [1971].

3. Nonlinear Saturated Amplitudes

In the previous section we showed that the collisional electrostatic ion cyclotron instability could be important in the bottomside high latitude ionosphere. In this section we discuss a possible nonlinear mechanism that might saturate these modes. In the literature several nonlinear saturation mechanisms for the electrostatic ion cyclotron instability have been studied. Davidson (1972) has discussed large amplitude trapping effects which become important when $\omega_t \tau_c >> 1$ where $\omega_t = k_\parallel (e\phi/m_e)^{1/2}$ is the electron trapping frequency and $\tau_c = k_\parallel \Delta v$ is the wave correlation time, ϕ is the wavepotential, $\underline{k}$ is the wavevector, and Δv_p is the spread in wave phase velocities parallel to the magnetic field. Collisional effects will prevent strong electron trapping. Another mechanism is ion resonance broadening [Dum and Dupree, 1970]. In this work we extend Dum and Dupree's theory to the case of the collisional EIC instability. Physically, the effect of the turbulence generated by the instability may be interpreted as an enhanced ion viscosity. In this section we shall present only estimates of the saturation amplitudes for typical ionospheric parameters and not a comprehensive full F-region study.

The nonlinear dispersion relation for the electrostatic ion-cyclotron modes, including the effects of resonance broadening, may be obtained by substituting $\bar{\omega} \equiv \omega + i\Delta\omega^W$ in lieu of ω in the ion contribution to Eq. (3) [Dum and Dupree, 1970]. Here $\Delta\omega^W$ is the modification introduced by the effect of a spectrum of finite amplitude modes on the particle orbits (resonance broadening effect). Thus,

$$1 + \varepsilon_e^\ell(\underline{k}, \omega) + \varepsilon_i^{n\ell}(\underline{k}, \omega + i\Delta \omega^W) = 0 \tag{23}$$

is the nonlinear dispersion relation for the EIC modes, where ε_j^ℓ is the linear dielectric constant and $\varepsilon_j^{n\ell}$ is the nonlinear dielectric constant. We note that Dum and Dupree [1970] have shown the effect of resonance broadening is important only for ions in the EIC wave case. Hence the contribution coming from the resonance broadening effect on electrons has been ignored in the expression (23). One may obtain an estimate for the nonlinear saturated amplitudes of EIC modes from (23) by setting the nonlinear growth rate $\gamma^{n\ell}$

$$\gamma^{n\ell} = \gamma_k^{\ell} - \Delta\omega^{W} = 0 \tag{24}$$

where γ_k^{ℓ} is the linear growth rate of the mode with wavenumber k. For the EIC instability case, $\Delta\omega^W$ may be approximated as [Dum and Dupree, 1970],

$$\Delta\omega^{W} = (\omega - \Omega_i)[(\frac{n_1}{n_1^0})^2 - 1]^{1/2} \tag{25}$$

Here n_1 is the saturated nonlinear amplitude of the wave, and, n_1^0 is the threshold level of the nonlinear amplitude at which the resonance broadening effects assume importance. The expression for n_1^0 is

$$\frac{n_1^0}{n} = (\frac{T_i}{ZT_e})(\frac{\Omega_i}{k_\perp v_i})^2 \frac{(\omega_k - \Omega_i)}{\Omega_i[F_1(\mu_i)]^{1/2}}$$

$$= (\frac{T_i}{ZT_e}) \frac{1}{\mu_i(F_1)^{1/2}} (\frac{\omega - \Omega_i}{\Omega_i}) \tag{26}$$

where $$F_1(x) = \begin{cases} \frac{1}{4}[1 - \frac{1}{4}(\frac{x}{2})^4 + \frac{1}{9}(\frac{x}{2})^6 + \dots, & \text{for } x \le 2 \\ \frac{1}{\pi x} & x \ge 3 \end{cases}$$

It may be noted that the broadening of resonances above corresponds to an enhancement in the group of ions that can exchange energy with the wave via resonance interaction. Stabilization of the mode results when the resonance is broadened to an extent such that the bulk of the ion distribution interacts with the wave and absorbs energy from it, thereby, leading to a steady finite amplitude nonlinear state. We now use expressions (24)-(25), to compute the nonlinear saturated amplitudes for the collisional EIC modes. From (24) and (25), one has

$$(\omega - \Omega_i)[(\frac{n_1}{n_1^0})^2 - 1]^{1/2} = \gamma_k^{\ell} \tag{27}$$

which leads to

$$(\frac{n_1}{n})^2 = (\frac{n_1^0}{n})^2[1 + \frac{(\gamma_k^{\ell})^2}{(\omega - \Omega_i)^2}] \tag{28}$$

or

$$\left(\frac{n_1}{n}\right)^2 = \frac{\left(\frac{T_i}{T_e}\right)^2\left(\frac{\Omega_i}{k_\perp v_i}\right)^4\left(\frac{\omega_r-\Omega_i}{\Omega_i}\right)^2}{F_1\left(\frac{k_\perp v_\perp}{\Omega_i}\right)}\left[1 + \frac{\left\{\frac{T_e}{T_i}\,\Omega_i\Gamma_1\,\frac{\nu_e}{k_\parallel^2 v_e^2}\,(k_\parallel V_d - \omega_r) - k_\perp^2\rho_i^2\nu_{ii} - \nu_{in}\right\}^2}{(\omega_r - \Omega_i)^2}\right] \tag{29}$$

using (17) and including ν_{ii} collisions.

For the case, $T_e = T_i$, one has

$$(\omega - \Omega_i) = \Omega_i\Gamma_1$$

which leads to

$$\left(\frac{n_1}{n}\right)^2 = \frac{\left(\frac{\Omega_i}{k_\perp v_i}\right)^4\Gamma_1^2}{F_1\left(\frac{k_\perp v_\perp}{\Omega_i}\right)}\left[1 + \left\{\frac{\nu_e}{k_\parallel^2 v_e^2}\,(k_\parallel V_d - \omega_r) - \frac{k_\perp^2\rho_i^2\nu_{ii} - \nu_{in}}{\Omega_i}\right\}^2\right] \tag{30}$$

The expression (30) gives the nonlinear saturated amplitudes of density fluctuations associated with the collisional ion-cyclotron modes due to resonance broadening effects in the presence of both electron (ν_e), ion-ion (ν_{ii}) and ion-neutral(ν_{in}) collisions applicable to bottomside ionospheric altitudes. A comparison with the collisionless case, discussed by Dum and Dupree [1970], shows that the saturated amplitudes can be higher in the collisional case, by an increment of approximately $\sim \frac{1}{2}[(V_d/V_e)(1/k_\parallel\lambda_e)]^2$. We note that, in the above comparison, it is implied that $\gamma_{kc}/(\omega_k - \Omega_i) << 1$, where γ_{kc} is the collisionless growth rate.

4. Summary and Discussion

In this study we have presented a comprehensive treatment of the theory of the electrostatic ion cyclotron instability in the collisional bottomside ionosphere. We have derived the linear dispersion relations for the ion cyclotron instability including both electron and ion collisions and solved analytically the dispersion relation in three limits: collisionless, weakly collisional, and collisional. In addition, we have solved the linear dispersion relation exactly using numerical methods using

parameters typical of the high latitude bottomside ionosphere. We note that the linear growth rates in the bottomside collisional regime can be of the same order as the corresponding topside collisionless growth rates. We have considered three cases corresponding to three different ionospheric conditions. The normal ionosphere is bracketed by two others with minimum density around 10^4 cm^{-3} at the lower end and maximum peak density of 10^6 cm^{-3} at the high end. The former represents a weakly collisional case ($\nu_e/\Omega_e < 10^{-4}$) and this can be considered as an extension of the previous collisionless EIC instability theories, the latter represents disturbed conditions, yielding high electron collisions and ion collisions. We have also considered pure O^+ and pure NO^+ plasmas and solved the dispersion relation for single species in both cases. We arrive at the following conclusions based on the linear calculation.

a. Given the realistic ionospheric parameters, we find that the theory of collisionless EIC instability (Kindel and Kennel, 1971) can not be extended to the bottomside F region (z < 400 km). Since, the critical drift velocities and growth rates are sensitve to n_e and T_e/T_i, a theory of collisional EIC using self-consistent collision frequencies and T_e/T_i should be used for accurate prediction of EIC excitation.

b. Electron collisions destabilize the EIC wave which results in higher growth rates. However, the ion-ion collisions damp the modes, the damping being equal to ν_{ii} in $k_\perp\rho_i >> 1$ limit and $\nu_{ii}k_\perp^2\rho_i^2/2$ in the $k_\perp\rho_i << 1$ limit. The EIC instability growth rate maximizes for $k_\perp\rho_i \gtrsim 1$.

c. For realistic profiles of the ionosphere, the collisional EIC wave growth rates are reduced by ion-neutral collisions in the bottomside F region and by ion-ion collisions above 300km, as expected.

d. For profiles given in Fig. 1, the collisionless theory (ion collisions dominate electron collisions) prevails for curve A and collisional theory (electron collisions are stronger and dominate ion collisions) prevails for curve C.

e. The growth rate maximizes in the weakly collisional (curve A, Fig. 1) regime at an altitude of 400 km and in the strongly collisional (curve C, Fig. 1) regime at an altitude of 250 km. In the collisional domain, (curve C, Fig 6) the growth rate has minimum at an altitude of 300 km and achieves a further lower value at E region altitudes (150 km or less).

f. The critical drift velocity required to excite the EIC waves is sensitive to the electron densites and thus are quite different in the collisionless and collisional domains. It is smaller at higher altitudes, z < 400 km, and larger at lower altitudes, z < 200 km.

g. For realistic ionospheric profiles, the growth rate is weakly dependent on the mass ratio (m_e/m_i). However, we find that the critical drift velocity is much smaller for EIC waves corresponding to gyrofrequencies of heavier ions than the critical drift corresponding to lighter ion (H^+) EIC wave excitation. Our single species calculation shows that NO^+ or O_2^+ EIC instability are much easier to excite than O^+ or H^+ EIC instability. Thus, in a multi-component plasma EIC waves at NO^+ will be first excited before, for example, O^+ EIC waves and in the bottomside ionosphere EIC instability at H^+ gyrofrequency is unlikely to be excited.

In addition, we have discussed a nonlinear saturation mechanism for the electrostatic ion cyclotron instability in the collisional regime based upon Dupree's ion resonance broadening theory. Dupree's resonance broadening theory is valid only for a broad spectrum of waves which are assumed isotropic and incoherent, i.e., the wave coherence time (spectral width) is much shorter than an ion cyclotron period. For a narrow (coherent) wave spectrum, resonance broadening theory must be replaced by an analysis which considers exact ion dynamics in a coherent wave [Davidson, 1972; Aamodt, 1970]. Recent nonlinear numerical simulations [Pritchett et al., 1981; Okuda and Ashour-Abdalla, 1981] of the collisionless ion cyclotron instability indicate a large amplitude coherent wave spectrum in the nonlinear regime. However these simulations also show several modes excited in the saturation phase of the ion cyclotron

instability. To our knowledge, there have been no nonlinear simulations of the collisional current-driven ion cyclotron instability. We shall now discuss some particular examples of the auroral ionospheric application of the collisional EIC instability.

In a recent study using sounding rockets, Yau et al. (1983) have recorded O^+ waves and strong perpendicular ion acceleration (ion conics) events at low altitudes (400-600 km) in the high latitude ionosphere during the expansive phase of an auroral substorm. Large relative density fluctuations ($\lesssim$ 10%) were also recorded near the ion conic acceleration regions. One major candidate for conic formation is EIC wave heating [Ungstrup et al., 1979; Okuda and Ashour-Abdalla, 1981]. Considering typical high latitude parameters, i.e., $T_e = T_i = 0.1$ eV, electron density corresponding to curve A of Fig. 1, ($n_e \sim 3 \times 10^4$, $\nu_e/\Omega_e \sim 2 \times 10^{-5}$, $\nu_i/\Omega_i \sim 7 \times 10^{-3}$) the growth rate of O^+ EIC waves, with $\lambda_\perp \sim 11$m ($k_\parallel \rho_i \sim 1.4$, $\rho_i \sim 2.56$m for O^+ ions) and $\lambda_\parallel \sim 200$ m, is $0.07\ \Omega_i$ or 21 sec^{-1}, taking Ω_i for O^+ in a 0.5 Gauss magnetic field as 300 Hz (Fig. 6, curve A). The corresponding growth rate for NO^+ EIC waves ($\lambda_\perp \sim 15$m) is $0.08\ \Omega_i$ or 12 sec^{-1}, taking Ω_i to be 150 Hz. The critical drift velocities can be read off Fig. 7 for O^+ ions. For the above parameters the critical drift velocity at an altitude of 300 km, for example, is $0.09\ V_e$ (Curve A, quiet conditions) which corresponds to 53 $\mu A/m^2$ for $n_e \sim 3 \times 10^{10}/m^3$. For NO^+ ions, under the same conditions, the critical drift velocity is $\sim 0.06\ V_e$ (Fig. 9) which corresponds to $40 \mu A/m^2$. For other profiles, Curves B (normal conditions) and C (disturbed conditions) of Fig 1 critical drift velocities are higher and require currents > 100 $\mu A/m^2$ and $\sim 1000 \mu A/m^2$, respectively. In view of these results we find that the ionospheric conditions corresponding to curve A of Fig. 1 are most conducive to EIC excitation at NO^+ and O_2^+ gyrofrequencies. From equation (30), the saturated amplitude for typical parameters i.e.,
$T_e = T_i = 0.1$ eV, $\Omega_i = 3 \times 10^2$ sec^{-1}, $\nu_e = 10^{-4}$ sec^{-1},
$\nu_{in}/\Omega_i = 10^{-3}$, $\nu_{ii}/\Omega_i \sim 10^{-2}$ is found to be approximately $n_1/n_0 = 0.24$ according to ion resonance-broadening theory for $k_\perp \rho_i = 1.2$, $k_\parallel/k_\perp = 0.1$, and $V_d \geq 2 \times 10^6$ cm/sec. We note that the saturation amplitude n_1/n_0 of EIC waves in the collisionless regime, using Eq. (30), is slightly smaller ($n_1/n_0 = .22$) than the collisional case.

Compelling evidence of the presence of energetic heavy ionspheric ions at high altitudes (> 1000 km) (Hultqvist, 1983; Klumpar et al., 1984; Yau et al., 1984) leads one to suggest that the bottomside ionosphere, which is a source of heavy ions, is indeed acting as an accelerating region for these heavy ions (Hultqvist, 1983). Furthermore, energetic heavy ions, NO^+ and O_2^+, have been observed at outer magnetospheric altitudes on days of high geomagnetic activity (Klecker et al., 1985; Craven et al., 1985). High geomagnetic activity at higher altitudes is usually indicative of a disturbed ionosphere, which could sustain large ionospheric currents that drive collisional EIC waves in the bottomside ionospher unstable. Thus, we conjecture that the ion cyclotron instability at the ion (heavy) cyclotron frequency, driven unstable by parallel field-aligned currents may selectively accelerate the NO^+, O_2^+ and O^+ ions in the transverse direction at low altitudes and these transversely accelerated ions form the heavy ion conics at the higher altitudes.

ACKNOWLEDGMENTS

This work was supported by the Defense Nuclear Agency, the National Aeronautics and Space Administration, and by the Office of Naval Research. We wish to thank C.L. Rino of SRI International for providing the Sondrestrom data. We thank G. Ganguli and Y.C. Lee for useful discussions.

Compelling evidence of the presence of energetic heavy ionspheric ions at high altitudes (> 1000 km) (Hultqvist, 1983; Klumpar et al., 1984; Yau et al., 1984) leads one to suggest that the bottomside ionosphere, which is a source of heavy ions, is indeed acting as an accelerating region for these heavy ions (Hultqvist, 1983). Furthermore, energetic heavy ions, NO^+ and O_2^+, have been observed at outer magnetospheric altitudes on days of high geomagnetic activity (Klecker et al., 1985; Craven et al., 1985). High geomagnetic activity at higher altitudes is usually indicative of a disturbed ionosphere, which could sustain large ionospheric currents that drive collisional EIC waves in the bottomside ionospher unstable. Thus, we conjecture that the ion cyclotron instability at the ion (heavy) cyclotron frequency, driven unstable by parallel field-aligned currents may selectively accelerate the NO^+, O_2^+ and O^+ ions in the transverse direction at low altitudes and these transversely accelerated ions form the heavy ion conics at the higher altitudes.

ACKNOWLEDGMENTS

This work was supported by the Defense Nuclear Agency, the National Aeronautics and Space Administration, and by the Office of Naval Research. We wish to thank C.L. Rino of SRI International for providing the Sondrestrom data. We thank G. Ganguli and Y.C. Lee for useful discussions.

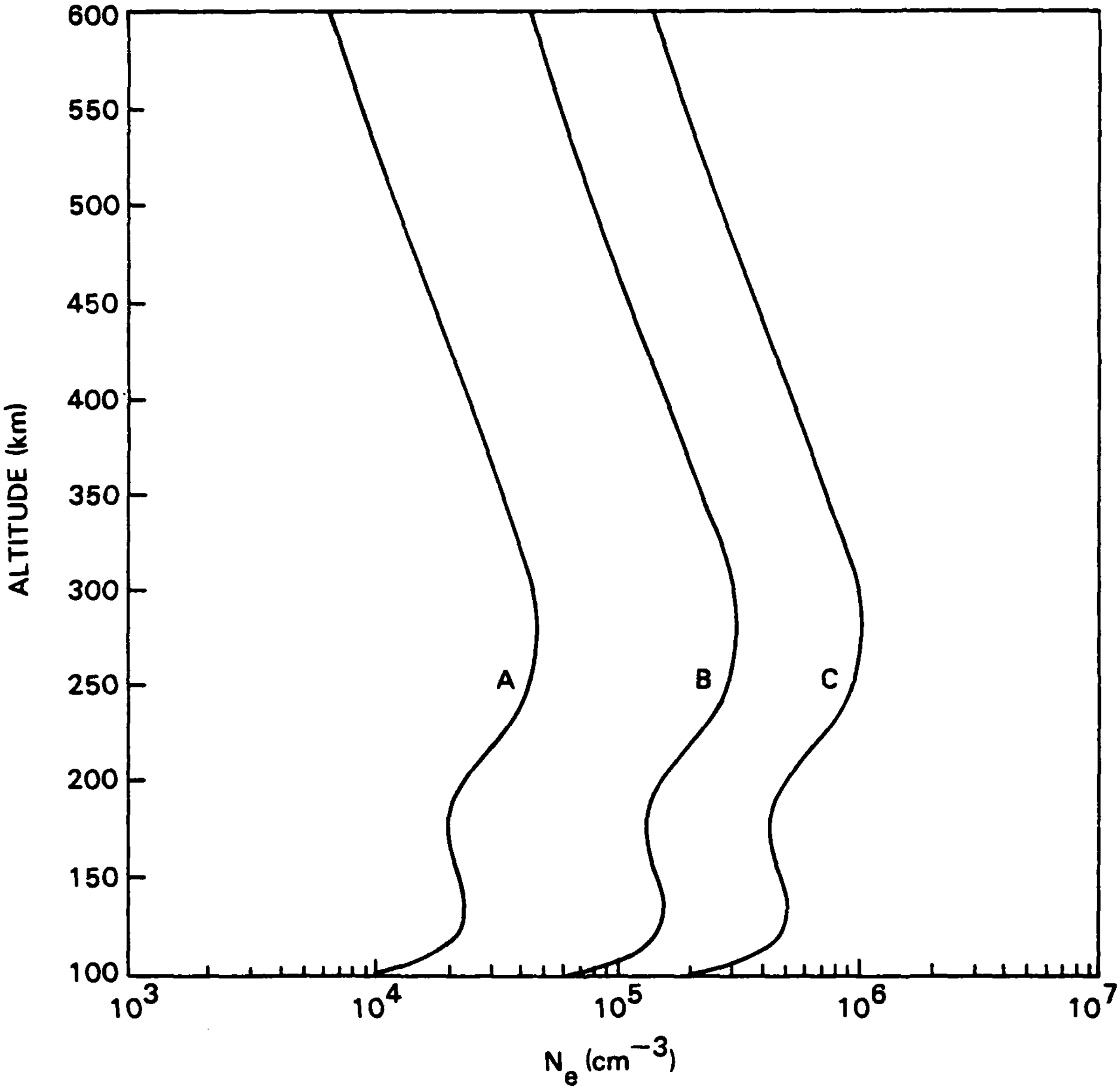

Fig. 1 Typical ionospheric electron density profiles based on Sondrestrom incoherent scatter radar data. Curve A represents a quiet condition, curve B an intermediate electron density, and curve C a disturbed condition.

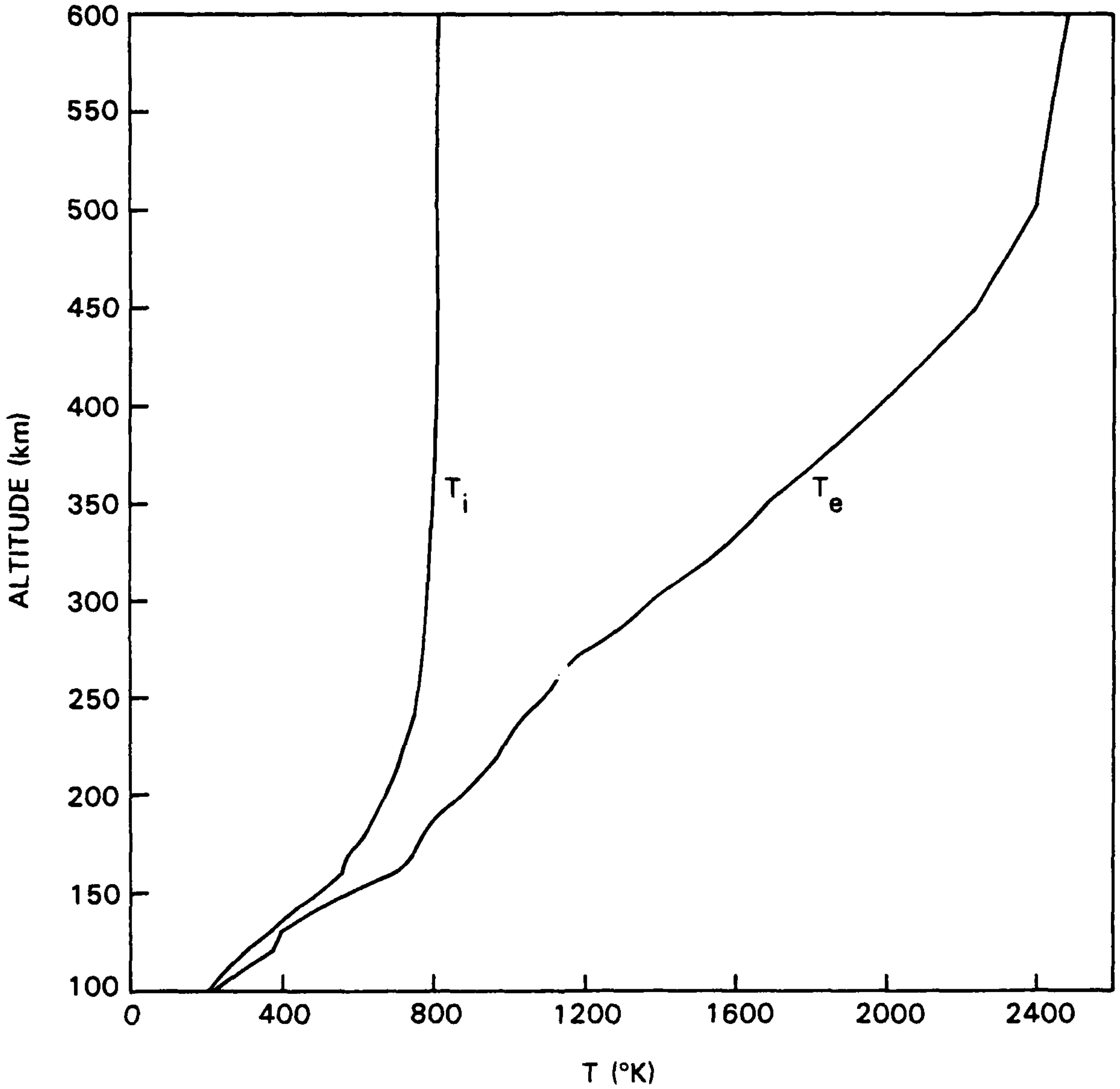

Fig. 2 Typical temperature profiles for T_e and T_i vs. altitude, based on Sondrestrom data.

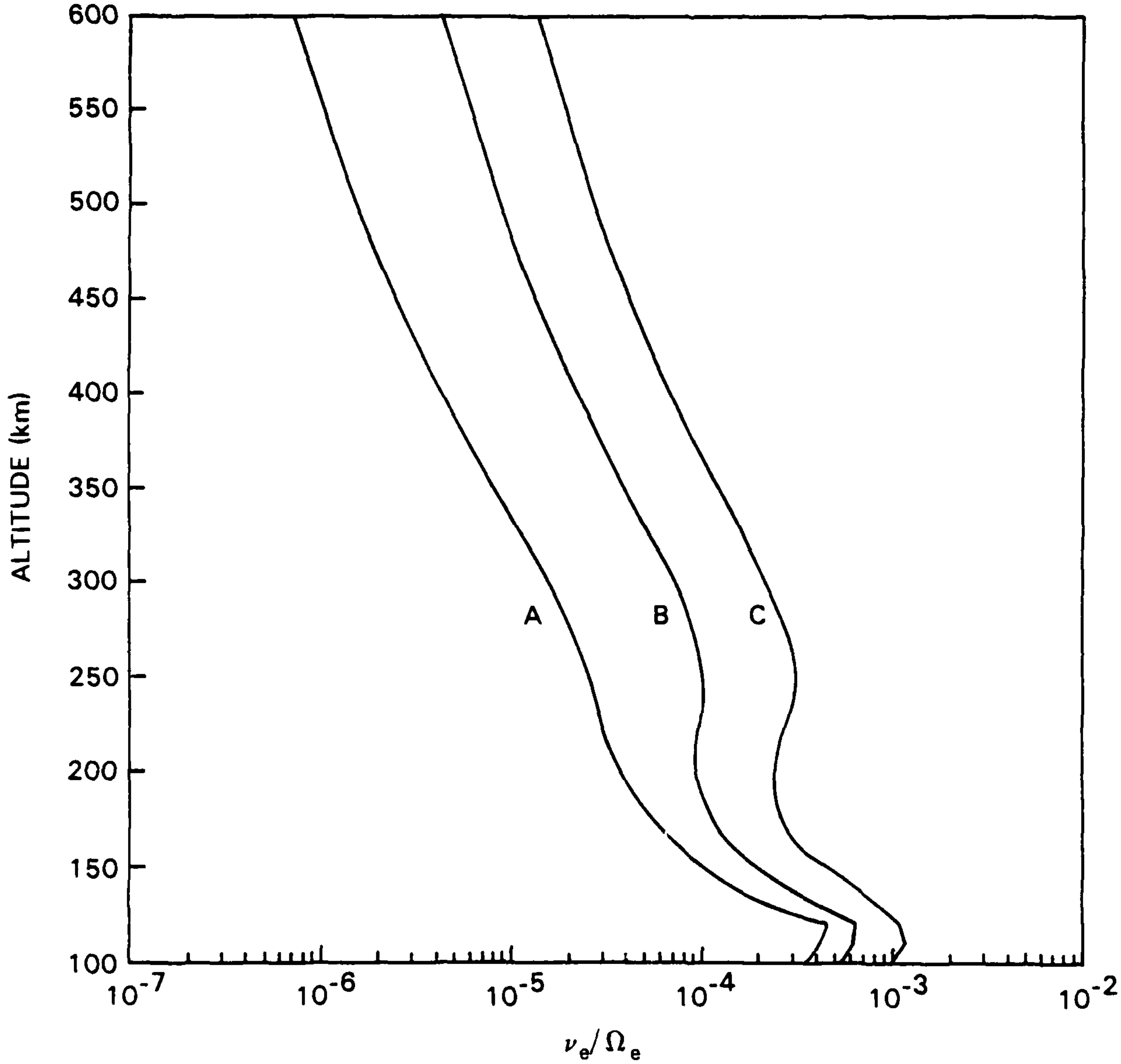

Fig. 3 Total electron collision frequencies(ν_e/Ω_e) where $(\nu_e = \nu_{en} + \nu_{ei})$ vs. altitude.

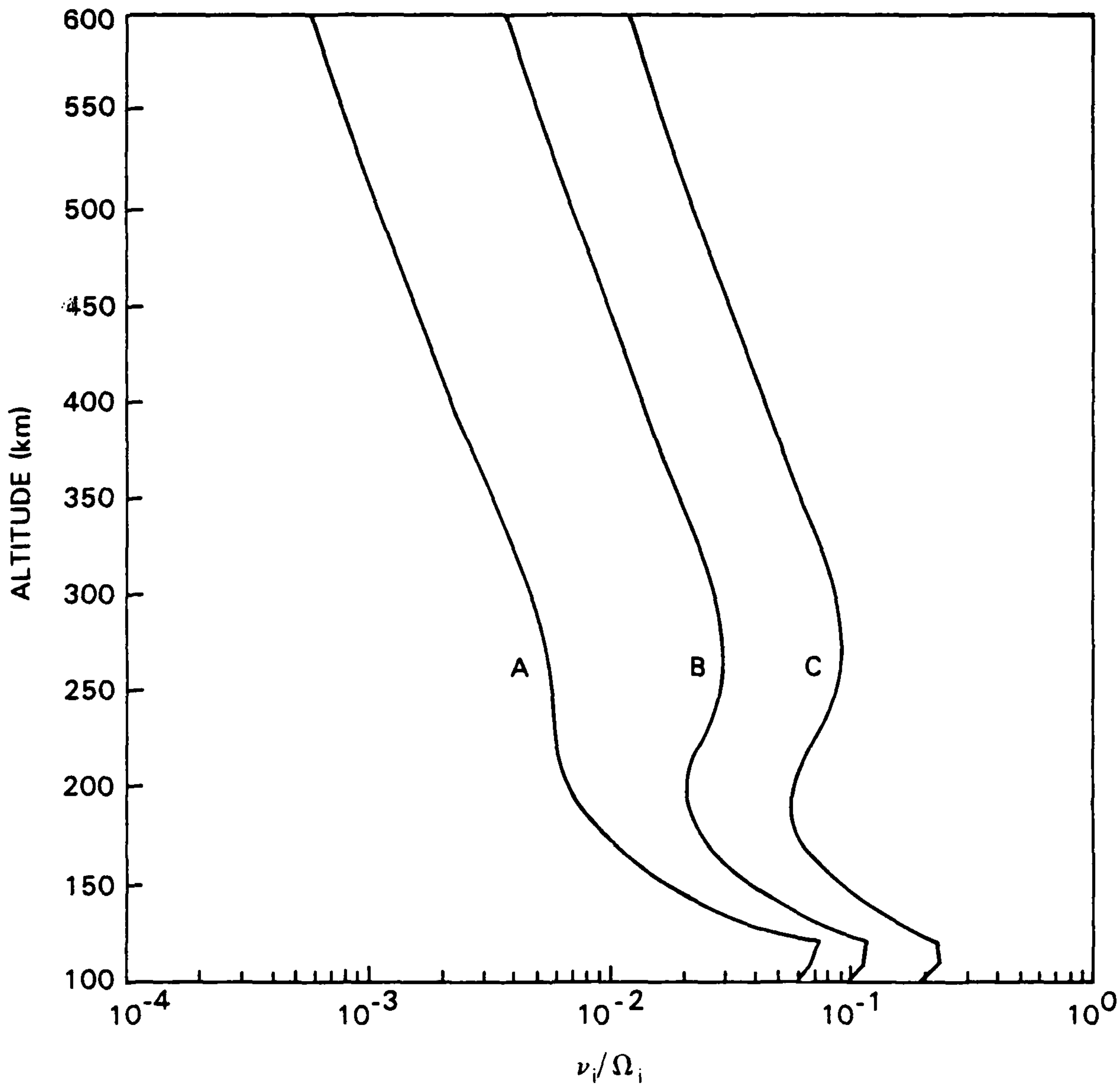

Fig. 4 Total ion collision frequencies ($\nu_i = \nu_{in} + \nu_{ii}$) with neutrals ($\nu_{in}$) and ions ($\nu_{ii}$) vs. altitude.

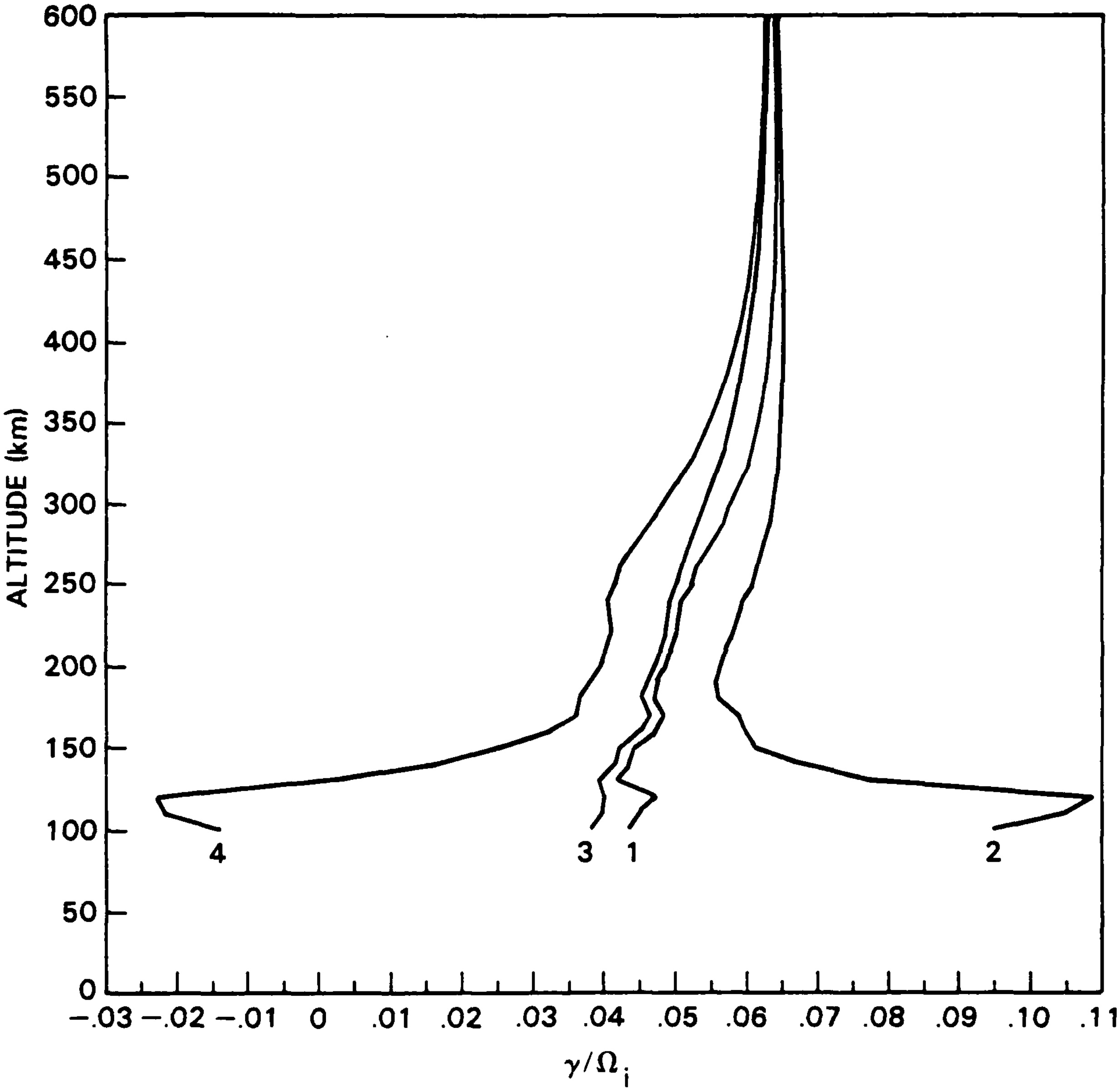

Fig. 5 Growth rate γ/Ω_i of electrostatic ion cyclotron instability vs. altitude for O^+ ion plasma using curve B of Fig. 1 and taking τ as varying with altitude and $\nu_e = \nu_i = 0$ (curve 1); $\nu_e = \nu_e(z)$, $\nu_i = 0$ (curve 2); $\nu_e = \nu_e(z)$, $\nu_i = \nu_i(z)$ (curve 3); and $\nu_e = 0$, $\nu_i = \nu_i(z)$ (curve 4). Here $k_\parallel/k_\perp = 0.06$, $k_\perp\rho_i = \sqrt{2}$ and $V_d/V_e = 0.3$.

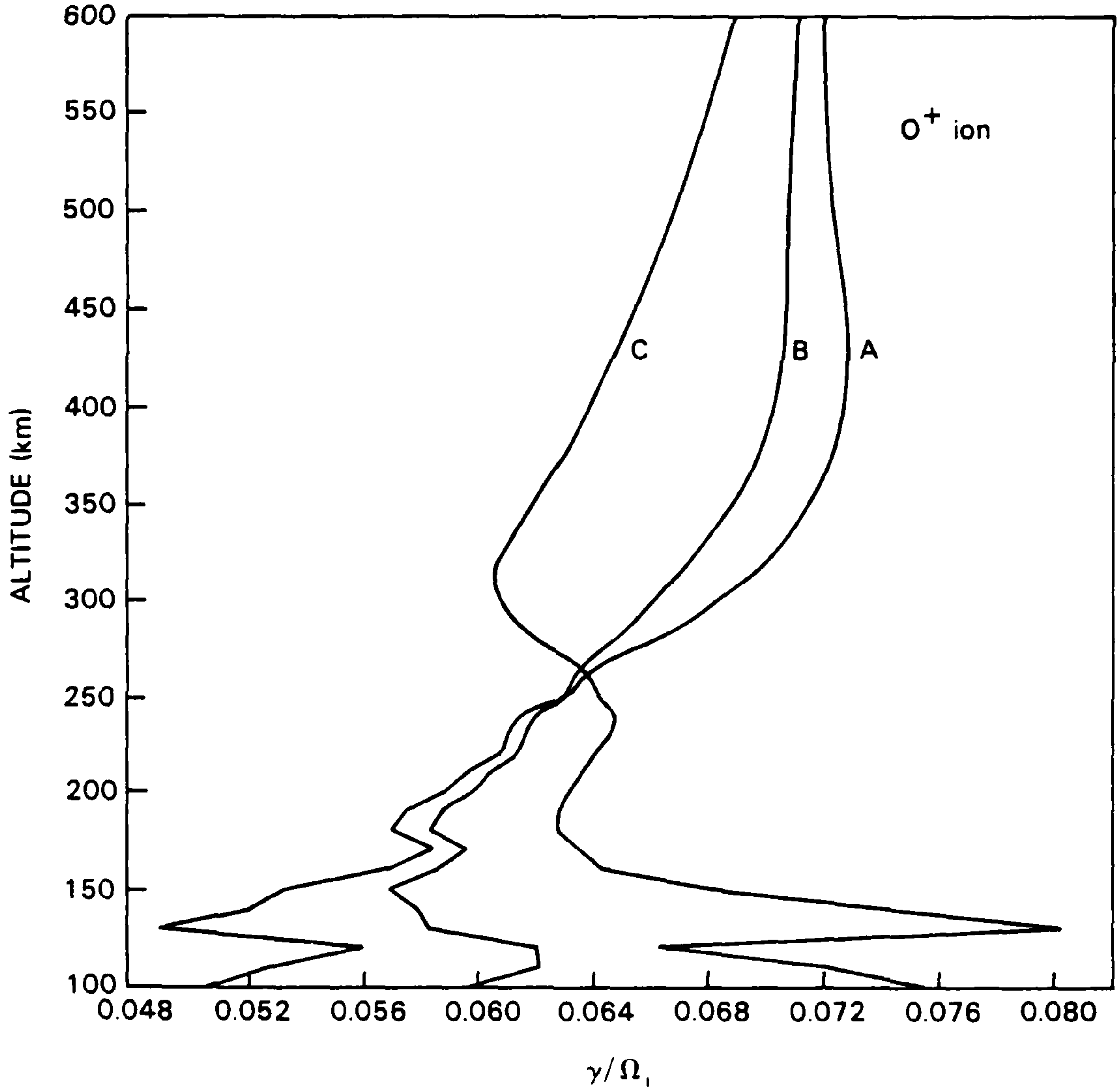

Fig. 6 Growth rate γ/Ω_i of electrostatic ion cyclotron instability vs. altitude for O^+ ion plasma using curves A-C of Fig. 1 with fixed parameters $k_\parallel/k_\perp = 0.06$, $k_\perp\rho_i = \sqrt{2}$ and $V_d/V_e = 0.3$.

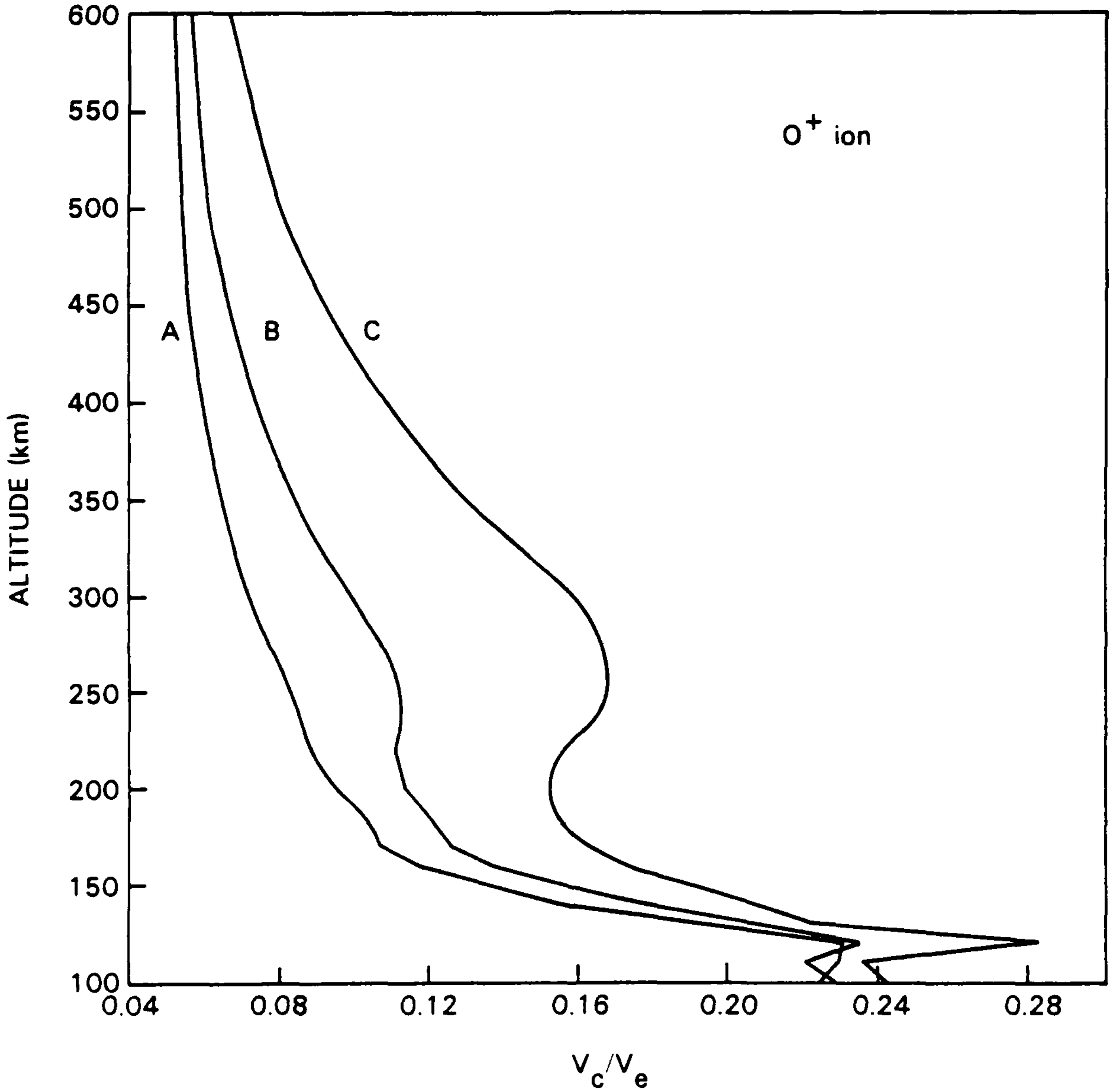

Fig. 7 Critical current drift velocity (V_c/V_e) for excitation of electrostatic ion cyclotron instability vs. altitude for curves A-C of Fig. 1 for O^+ ion plasma and $k_\parallel/k_\perp = 0.06$, $k_\perp\rho_i = \sqrt{2}$.

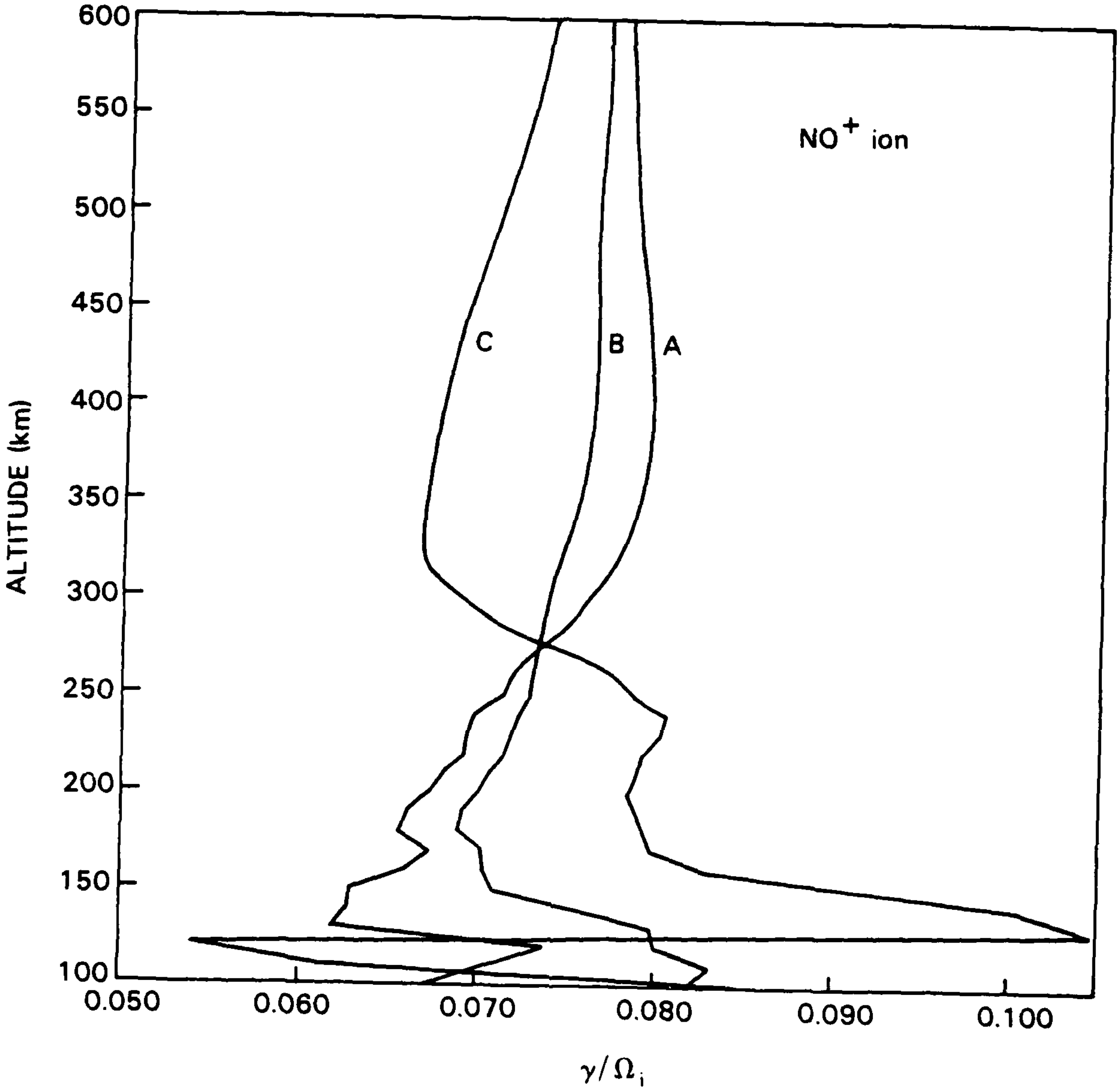

Fig. 8 Growth rate γ/Ω_i of electrostatic ion cyclotron instability vs. altitude for NO^+ ion plasma using curves A-C of Fig. 1 with fixed parameters $k_\parallel/k_\perp = 0.06$, $k_\perp\rho_i = \sqrt{2}$ and $V_d/V_e = 0.3$.

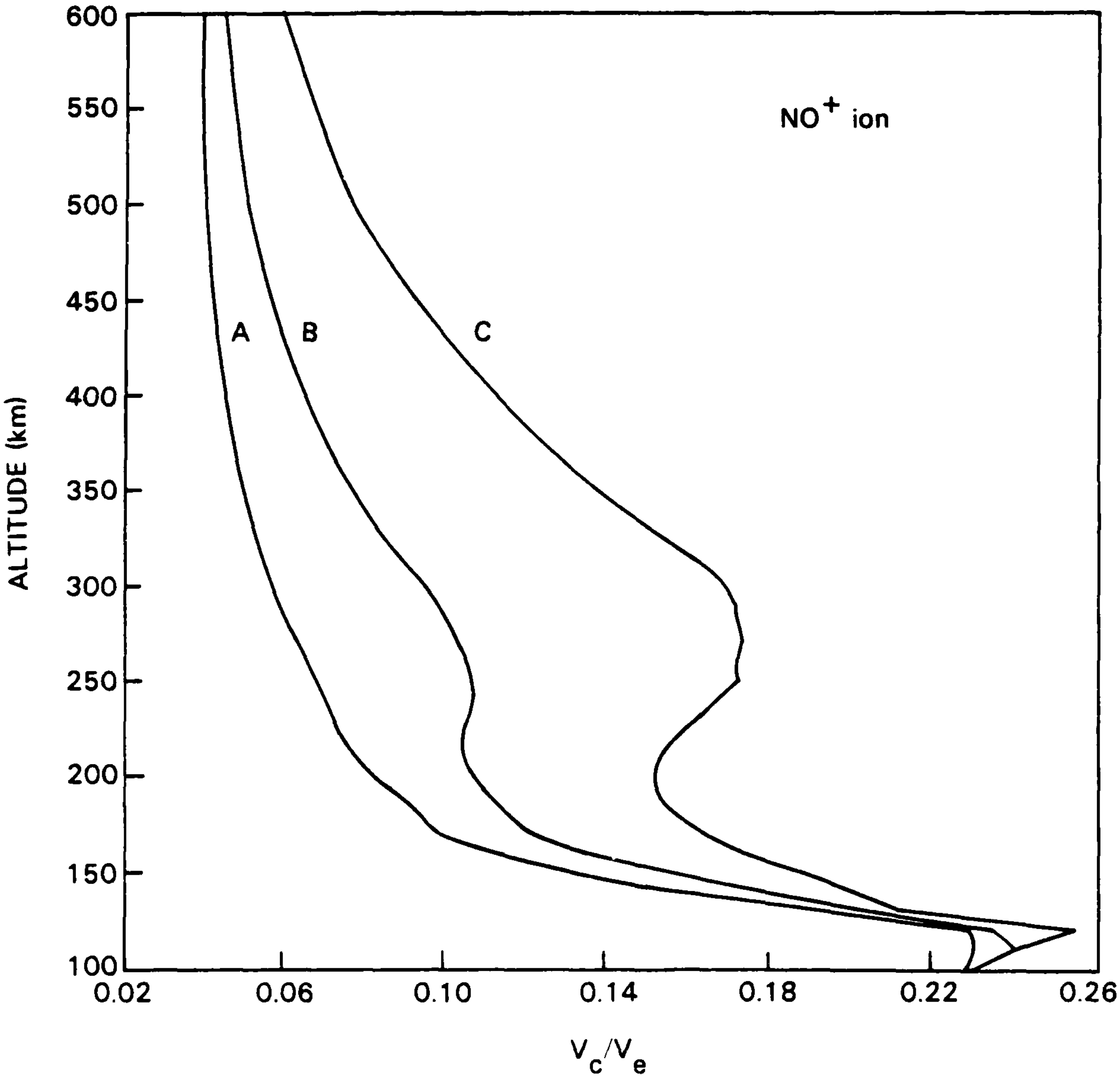

Fig. 9 Critical current drift velocity (V_c/V_e) for excitation of electrostatic ion cyclotron instability vs. altitude for curves A-C of Fig. 1 for NO^+ ion plasma and $k_\parallel/k_\perp = 0.06$, $k_\perp \rho_i = \sqrt{2}$.

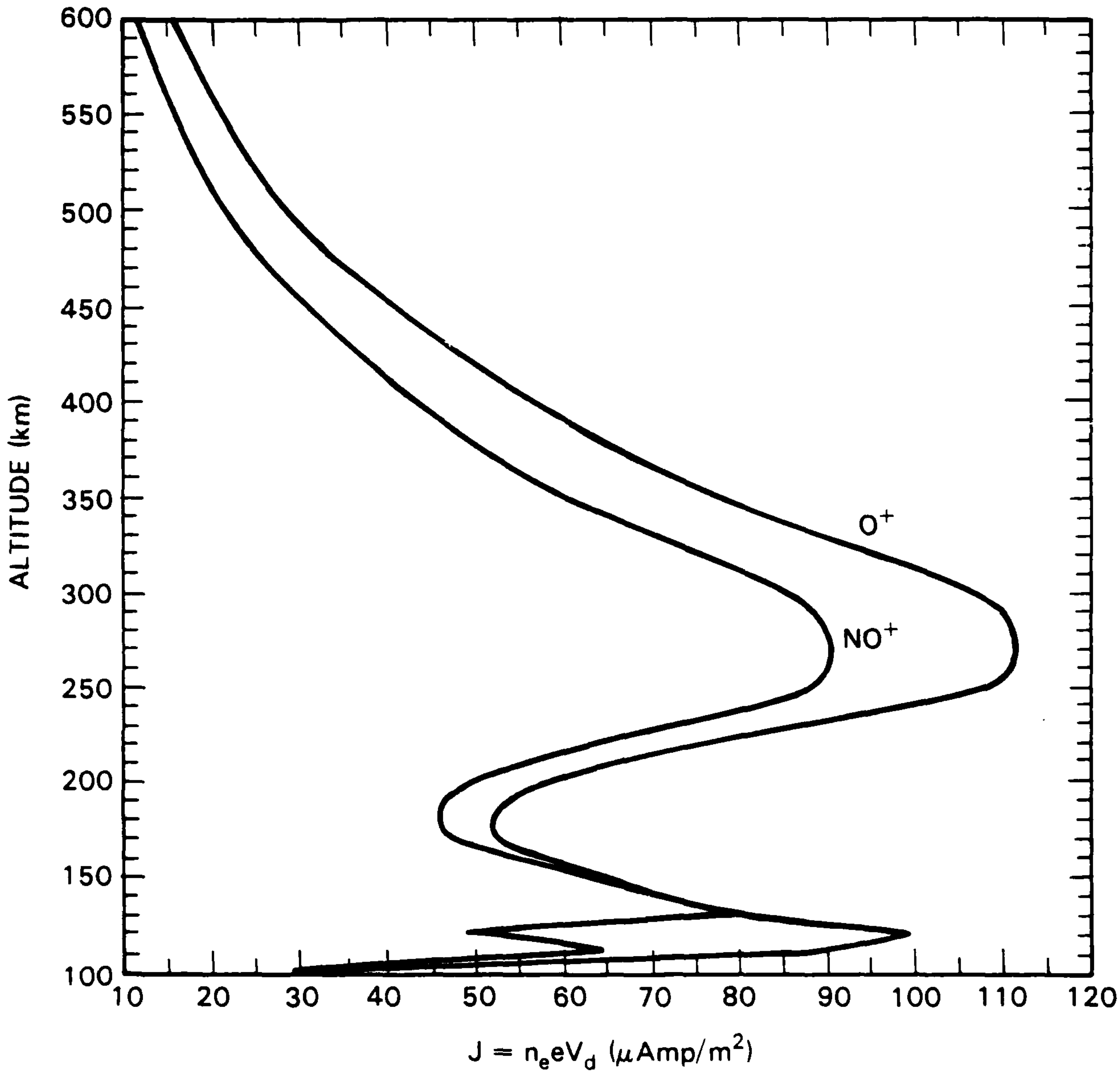

Fig. 10 Threshold currents in $\mu A/m^2$ required to excite O^+ and NO^+ EIC waves in O^+ and NO^+ plasmas, respectively. The critical currents are calculated for $J = n_e\ e\ V_d$ using V_c/V_e from curves A of Figs. 7 and 9, n_e from curve A of Fig. 1 and T_e from Fig. 2. The parameters used are $k\rho_i = \sqrt{2}$ and $k_\parallel/k_\perp = 0.06$.

REFERENCES

Aamodt, R.E., Particle motion in the presence of three dimensional finite amplitude harmonic cyclotron waves, Phys. Fluids., 13, 2341, 1970.

Banks, P.M. and G. Kockarts, Aeronomy, Academic Press, New York, 1973, Vol. A and B.

Bering, E.A., The plasma wave environment of an auroral arc: Electrostatic ion cyclotron waves in the diffuse aurora, J. Geophys. Res., 89, 1635, 1984.

Bythrow, P.F., T.A. Potemra, W.B. Hanson, L.J. Zanetti, C.-I. Meng, R.E. Huffmann, F.J. Rich and D.A. Hardy, Earthward directed high density Birkeland currents observed by HILAT, J. Geophys. Res., 89, 9114, 1984.

Chaturvedi, P.K. and P.K. Kaw, Current driven ion cyclotron waves in collisional plasma, Plasma Phys., 17, 447, 1975.

Chaturvedi, P.K., Collisional ion cyclotron waves in the auroral ionosphere, J. Geophys. Res., 81, 6169, 1976.

Chaturvedi, P.K., P. Satyanarayana, G. Ganguli, M.J. Keskinen, and J.D. Huba, Local and Nonlocal Theories of Collisional Current Driven Ion Cyclotron Instability, Bull. Am. Phy. Soc., 29, 1192, 1984.

Clemmow, P.C. and J.P. Dougherty, Electrodynamics of Particles and Plasmas, Addison-Wesley, Reading, Mass., 1969.

Craven, P.D, R.C. Olsen, C.R. Chappel, and L. Kakani, Observations of molecular ions in the Earth's magnetosphere, J. Geophys. Res., 90, xxxx, 1985.

D'Angelo, N., Type 3 spectra of the radar aurora, J. Geophys. Res., 78 3587, 1973.

Davidson, R.C., Methods in Nonlinear Plasma Theory, Academic, New York, 1972.

Drummond, W.E. and M.N. Rosenbluth, Anomalous diffusion arising from microinstabilities in a plasma, Phys. Fluids, 5, 1507, 1962.

Dum, C.T. and T.H. Dupree, Nonlinear stabilization of high frequency instabilities in a magnetic field, Phys. Fluids, 13, 2064, 1970.

Dupree, T.H., A perturbation theory for strong plasma turbulence, Phys. Fluids, 9, 1773, 1966.

Fejer, B.G., R.W. Reed, D.T. Farley, W.E. Swartz and M.C. Kelley, Ion cyclotron waves as a possible source of resonant auroral radar echoes, J. geophys. Res., 89, 187, 1984.

Ganguli, G., P. Palmadesso and Y.C. Lee, A new mechanism for excitation of electrostatic ion-cyclotron waves and associated perpendicular heating, submitted to Geophys. Res. Lett., 13, xxxx, 1985.

Hoffman, J. H., W.H. Dodson, C.R. Lippincott, and H.D. Hammack, Initial ion composition results from the Isis-2 satellite, J. Geophys. Res., 79, 4246, 1974.

Hultqvist, B., On the origin of hot ions in the disturbed dayside magnetosphere, Planet. Space Sci., 37, 173, 1983

Kelly, J.D., Sondrestrom radar - initial results, Geophys. Res. Lett., 10, 1112, 1983

Kindel, J.M. and C.F. Kennel, Topside current instabilities, J. Geophys. Res., 76, 3055, 1971.

Kintner, P.M., M.C. Kelley, and F.S. Mozer, Electrostatic hydrogen cyclotron waves near one earth radius altitude in the polar magnetosphere, Geophy. Res. Lett., 5, 139, 1978.

Kintner, P.M., M.C. Kelley, R.D. Sharp, A.G. Shielmetti, M. Temerin, C. Cattell, P.F. Mizera, and J.F. Fennell, Simultaneous observations of energetic (keV) upstreaming ions and electrostatic hydrogen cyclotron waves, j. Geophys. Res., 84, 7201, 1979.

Klecker, B., D. Hovestadt, E. Mobius, M. Scholer, G. Gloecker, and F. M. Ipavich, Observation of energetic molecular ions in the outer magnetosphere, paper presented at the Chapman Conference on Ion Acceleration in the magnetosphere and Ionosphere, Wellesley College, Wellesley, Mass., June 3-7, 1985.

Klumpar, D.M., W.K. Peterson, and E.G. Shelly, Direct evidence for two stage (bimodel) acceleration of ionospheric ions, J. Geophys. Res, 89, 10779, 1984.

Levine, A.M., and A.F. Kuckes, Excitation of electrostatic ion cyclotron oscillations, Phys. Fluids, 9, 2263, 1966.

Martelli, G., P.N. Collis, M. Giles and P.J. Christiansen, Optical detection of electrostatic ion cyclotron waves in the auroral plasma, Plante. Space Sci., 25, 643, 1977.

Milić, B., Spontanious excitation of long-wave ion-cyclotron and ion-acoustic oscillations in fully ionized plasmas, Phys. Fluids, 15, 1630, 1972.

Ogawa, T., H. Mori, S. Miyazaki, and H. Yamagishi, Electrostatic plasma instabilities in highly active aurora, Mem. Natl. Inst. Polar Res. Spec. Issue Japan, 18, 312, 1981.

Okuda, H. and M. Ashour-Abdulla, Formation of a conical distribution and intense ion heating in the preence of hydrogen cyclotron waves, Geophys. Res. Lett. 8, 811, 1981.

Petviashvili, V.I., Nonlinear oscillations and some effects due to a longitudinal current in a plasma, Zh. Eksp. Teor. Fiz. 45, 1467, 1963. [Sov. Phys. - JETP 18, 1014, 1964].

Pritchett, P.L., M. Ashour-Abdalla, and J.M. Dawson, Simulation of the current-driven electrostatic ion cyclotron instability, Geophys. Res. Lett. 8, 611,1981.

Spitzer, L., Physics of Fully Ionized Gases, Interscience, N.Y., 1962.

Ungstrup, E., D.M. Klumpar, and W. J. Heikkila, Heating of ions to superthermal energies in the topside ionosphere by electrostatic ion cyclotron waves, J. Geophys. Res, 84, 4289, 1979.

Varma, R.K. and D. Bhadra, Collisional effects in a hot plasma at ion gyro-frequency, Phys. Fluids, 7, 1082, 1964.

Yau, A.W., B.A. Whalen, A.G. McNamara, P.J. Kellogg, and W. Bernstein, Particle and wave observations of low-altitude ionospheric acceleration events, J. Geophys. Res., 88, 341, 1983.

Yau, A.W., B.A. Whalen, W.K. Peterson, and E.G. Shelly, Distribution of upflowing ionospheric ions in the high-altitude polar cap and auroral ionsopnere, J. Geophys. Res., 89 5507, 1984

DISTRIBUTION LIST

DEPARTMENT OF DEFENSE

ASSISTANT SECRETARY OF DEFENSE
COMM, CMD, CONT 7 INTELL
WASHINGTON, D.C. 20301

DIRECTOR
COMMAND CONTROL TECHNICAL CENTER
PENTAGON RM BE 685
WASHINGTON, D.C. 20301
  01CY ATTN C-650
  01CY ATTN C-312 R. MASON

DIRECTOR
DEFENSE ADVANCED RSCH PROJ AGENCY
ARCHITECT BUILDING
1400 WILSON BLVD.
ARLINGTON, VA. 22209
  01CY ATTN NUCLEAR
        MONITORING RESEARCH
  01CY ATTN STRATEGIC TECH OFFICE

DEFENSE COMMUNICATION ENGINEER CENTER
1860 WIEHLE AVENUE
RESTON, VA. 22090
  01CY ATTN CODE R410
  01CY ATTN CODE R812

DEFENSE TECHNICAL INFORMATION CENTER
CAMERON STATION
ALEXANDRIA, VA. 22314
  02CY

DIRECTOR
DEFENSE NUCLEAR AGENCY
WASHINGTON, D.C. 20305
  01CY ATTN STVL
  04CY ATTN TITL
  01CY ATTN DDST
  03CY ATTN RAAE

COMMANDER
FIELD COMMAND
DEFENSE NUCLEAR AGENCY
KIRTLAND, AFB, NM 87115
  01CY ATTN FCPR

DEFENSE NUCLEAR AGENCY
SAO/DNA
BUILDING 20676
KIRTLAND AFB, NM 87115
  01CY D.C. THORNBURG

DIRECTOR
INTERSERVICE NUCLEAR WEAPONS SCHOOL
KIRTLAND AFB, NM 87115
  01CY ATTN DOCUMENT CONTROL

JOINT CHIEFS OF STAFF
WASHINGTON, D.C. 20301
  01CY ATTN J-3 WWMCCS EVALUATION
        OFFICE

DIRECTOR
JOINT STRAT TGT PLANNING STAFF
OFFUTT AFB
OMAHA, NB 68113
  01CY ATTN JSTPS/JLKS
  01CY ATTN JPST G. GOETZ

CHIEF
LIVERMORE DIVISION FLD COMMAND DNA
DEPARTMENT OF DEFENSE
LAWRENCE LIVERMORE LABORATORY
P.O. BOX 808
LIVERMORE, CA 94550
  01CY ATTN FCPRL

COMMANDANT
NATO SCHOOL (SHAPE)
APO NEW YORK 09172
  01CY ATTN U.S. DOCUMENTS OFFICER

UNDER SECY OF DEF FOR RSCH & ENGRG
DEPARTMENT OF DEFENSE
WASHINGTON, D.C. 20301
  01CY ATTN STRATEGIC & SPACE
        SYSTEMS (OS)

COMMANDER/DIRECTOR
ATMOSPHERIC SCIENCES LABORATORY
U.S. ARMY ELECTRONICS COMMAND
WHITE SANDS MISSILE RANGE, NM 88002
  01CY ATTN DELAS-EO, F. NILES

DIRECTOR
BMD ADVANCED TECH CTR
HUNTSVILLE OFFICE
P.O. BOX 1500
HUNTSVILLE, AL 35807
01CY ATTN ATC-T MELVIN T. CAPPS
01CY ATTN ATC-O W. DAVIES
01CY ATTN ATC-R DON RUSS

PROGRAM MANAGER
BMD PROGRAM OFFICE
5001 EISENHOWER AVENUE
ALEXANDRIA, VA 22333
01CY ATTN DACS-BMT J. SHEA

CHIEF C-E- SERVICES DIVISION
U.S. ARMY COMMUNICATIONS CMD
PENTAGON RM 1B269
WASHINGTON, D.C. 20310
01CY ATTN C-E-SERVICES DIVISION

COMMANDER
FRADCOM TECHNICAL SUPPORT ACTIVITY
DEPARTMENT OF THE ARMY
FORT MONMOUTH, N.J. 07703
01CY ATTN DRSEL-NL-RD H. BENNET
01CY ATTN DRSEL-PL-ENV H. BOMKE
01CY ATTN J.E. QUIGLEY

COMMANDER
U.S. ARMY COMM-ELEC ENGRG INSTAL AGY
FT. HUACHUCA, AZ 85613
01CY ATTN CCC-EMEO GEORGE LANE

COMMANDER
U.S. ARMY FOREIGN SCIENCE & TECH CTR
220 7TH STREET, NE
CHARLOTTESVILLE, VA 22901
01CY ATTN DRXST-SD

COMMANDER
U.S. ARMY MATERIAL DEV & READINESS CMD
5001 EISENHOWER AVENUE
ALEXANDRIA, VA 22333
01CY ATTN DRCLDC J.A. BENDER

COMMANDER
U.S. ARMY NUCLEAR AND CHEMICAL AGENCY
7500 BACKLICK ROAD
BLDG 2073
SPRINGFIELD, VA 22150
01CY ATTN LIBRARY

DIRECTOR
U.S. ARMY BALLISTIC RESEARCH
LABORATORY
ABERDEEN PROVING GROUND, MD 21005
01CY ATTN TECH LIBRARY,
EDWARD BAICY

COMMANDER
U.S. ARMY SATCOM AGENCY
FT. MONMOUTH, NJ 07703
01CY ATTN DOCUMENT CONTROL

COMMANDER
U.S. ARMY MISSILE INTELLIGENCE AGENCY
REDSTONE ARSENAL, AL 35809
01CY ATTN JIM GAMBLE

DIRECTOR
U.S. ARMY TRADOC SYSTEMS ANALYSIS
ACTIVITY
WHITE SANDS MISSILE RANGE, NM 88002
01CY ATTN ATAA-SA
01CY ATTN TCC/F. PAYAN JR.
01CY ATTN ATTA-TAC LTC J. HESSE

COMMANDER
NAVAL ELECTRONIC SYSTEMS COMMAND
WASHINGTON, D.C. 20360
01CY ATTN NAVALEX 034 T. HUGHES
01CY ATTN PME 117
01CY ATTN PME 117-T
01CY ATTN CODE 5011

COMMANDING OFFICER
NAVAL INTELLIGENCE SUPPORT CTR
4301 SUITLAND ROAD, BLDG. 5
WASHINGTON, D.C. 20390
01CY ATTN MR. DUBBIN STIC 12
01CY ATTN NISC-50
01CY ATTN CODE 5404 J. GALET

COMMANDER
NAVAL OCEAN SYSTEMS CENTER
SAN DIEGO, CA 92152
01CY ATTN J. FERGUSON

NAVAL RESEARCH LABORATORY
WASHINGTON, D.C. 20375
 01CY ATTN CODE 4700 S.L. Ossakow,
 26 CYS IF UNCLASS
 (01CY IF CLASS)
 ATTN CODE 4780 J.D. HUBA, 50
 CYS IF UNCLASS, 01CY IF CLASS
 01CY ATTN CODE 4701 I. VITKOVITSKY
 01CY ATTN CODE 7500
 01CY ATTN CODE 7550
 01CY ATTN CODE 7580
 01CY ATTN CODE 7551
 01CY ATTN CODE 7555
 01CY ATTN CODE 4730 E. MCLEAN
 01CY ATTN CODE 4108
 01CY ATTN CODE 4730 B. RIPIN
 20CY ATTN CODE 2628

COMMANDER
NAVAL SPACE SURVEILLANCE SYSTEM
DAHLGREN, VA 22448
 01CY ATTN CAPT J.H. BURTON

OFFICER-IN-CHARGE
NAVAL SURFACE WEAPONS CENTER
WHITE OAK, SILVER SPRING, MD 20910
 01CY ATTN CODE F31

DIRECTOR
STRATEGIC SYSTEMS PROJECT OFFICE
DEPARTMENT OF THE NAVY
WASHINGTON, D.C. 20376
 01CY ATTN NSP-2141
 01CY ATTN NSSP-2722 FRED WIMBERLY

COMMANDER
NAVAL SURFACE WEAPONS CENTER
DAHLGREN LABORATORY
DAHLGREN, VA 22448
 01CY ATTN CODE DF-14 R. BUTLER

OFFICER OF NAVAL RESEARCH
ARLINGTON, VA 22217
 01CY ATTN CODE 465
 01CY ATTN CODE 461
 01CY ATTN CODE 402
 01CY ATTN CODE 420
 01CY ATTN CODE 421

COMMANDER
AEROSPACE DEFENSE COMMAND/DC
DEPARTMENT OF THE AIR FORCE
ENT AFB, CO 80912
 01CY ATTN DC MR. LONG

COMMANDER
AEROSPACE DEFENSE COMMAND/XPD
DEPARTMENT OF THE AIR FORCE
ENT AFB, CO 80912
 01CY ATTN XPDQQ
 01CY ATTN XP

AIR FORCE GEOPHYSICS LABORATORY
HANSCOM AFB, MA 01731
 01CY ATTN OPR HAROLD GARDNER
 01CY ATTN LKB
 KENNETH S.W. CHAMPION
 01CY ATTN OPR ALVA T. STAIR
 01CY ATTN PHD JURGEN BUCHAU
 01CY ATTN PHD JOHN P. MULLEN

AF WEAPONS LABORATORY
KIRTLAND AFT, NM 87117
 01CY ATTN SUL
 01CY ATTN CA ARTHUR H. GUENTHER
 01CY ATTN NTYCE 1LT. G. KRAJEI

AFTAC
PATRICK AFB, FL 32925
 01CY ATTN TN

AIR FORCE AVIONICS LABORATORY
WRIGHT-PATTERSON AFB, OH 45433
 01CY ATTN AAD WADE HUNT
 01CY ATTN AAD ALLEN JOHNSON

DEPUTY CHIEF OF STAFF
RESEARCH, DEVELOPMENT, & ACQ
DEPARTMENT OF THE AIR FORCE
WASHINGTON, D.C. 20330
 01CY ATTN AFRDQ

HEADQUARTERS
ELECTRONIC SYSTEMS DIVISION
DEPARTMENT OF THE AIR FORCE
HANSCOM AFB, MA 01731-5000
 01CY ATTN J. DEAS
 ESD/SCD-4

COMMANDER
FOREIGN TECHNOLOGY DIVISION, AFSC
WRIGHT-PATTERSON AFB, OH 45433
 01CY ATTN NICD LIBRARY
 01CY ATTN ETDP B. BALLARD

COMMANDER
ROME AIR DEVELOPMENT CENTER, AFSC
GRIFFISS AFB, NY 13441
 01CY ATTN DOC LIBRARY/TSLD
 01CY ATTN OCSE V. COYNE

STRATEGIC AIR COMMAND/XPFS
OFFUTT AFB, NB 68113
01CY ATTN ADWATE MAJ BRUCE BAUER
01CY ATTN NRT
01CY ATTN DOK CHIEF SCIENTIST

SAMSO/SK
P.O. BOX 92960
WORLDWAY POSTAL CENTER
LOS ANGELES, CA 90009
01CY ATTN SKA (SPACE COMM SYSTEMS) M. CLAVIN

SAMSO/MN
NORTON AFB, CA 92409
(MINUTEMAN)
01CY ATTN MNNL

COMMANDER
ROME AIR DEVELOPMENT CENTER, AFSC
HANSCOM AFB, MA 01731
01CY ATTN EEP A. LORENTZEN

DEPARTMENT OF ENERGY
LIBRARY ROOM G-042
WASHINGTON, D.C. 20545
01CY ATTN DOC CON FOR A. LABOWITZ

DEPARTMENT OF ENERGY
ALBUQUERQUE OPERATIONS OFFICE
P.O. BOX 5400
ALBUQUERQUE, NM 87115
01CY ATTN DOC CON FOR D. SHERWOOD

EG&G, INC.
LOS ALAMOS DIVISION
P.O. BOX 809
LOS ALAMOS, NM 85544
01CY ATTN DOC CON FOR J. BREEDLOVE

UNIVERSITY OF CALIFORNIA
LAWRENCE LIVERMORE LABORATORY
P.O. BOX 808
LIVERMORE, CA 94550
01CY ATTN DOC CON FOR TECH INFO DEPT
01CY ATTN DOC CON FOR L-389 R. OTT
01CY ATTN DOC CON FOR L-31 R. HAGER

LOS ALAMOS NATIONAL LABORATORY
P.O. BOX 1663
LOS ALAMOS, NM 87545
01CY ATTN DOC CON FOR J. WOLCOTT
01CY ATTN DOC CON FOR R.F. TASCHEK
01CY ATTN DOC CON FOR E. JONES
01CY ATTN DOC CON FOR J. MALIK
01CY ATTN DOC CON FOR R. JEFFRIES
01CY ATTN DOC CON FOR J. ZINN
01CY ATTN DOC CON FOR D. WESTERVELT
01CY ATTN D. SAPPENFIELD

SANDIA LABORATORIES
P.O. BOX 5800
ALBUQUERQUE, NM 87115
01CY ATTN DOC CON FOR W. BROWN
01CY ATTN DOC CON FOR A. THORNBROUGH
01CY ATTN DOC CON FOR T. WRIGHT
01CY ATTN DOC CON FOR D. DAHLGREN
01CY ATTN DOC CON FOR 3141
01CY ATTN DOC CON FOR SPACE PROJECT DIV

SANDIA LABORATORIES
LIVERMORE LABORATORY
P.O. BOX 969
LIVERMORE, CA 94550
01CY ATTN DOC CON FOR B. MURPHEY
01CY ATTN DOC CON FOR T. COOK

OFFICE OF MILITARY APPLICATION
DEPARTMENT OF ENERGY
WASHINGTON, D.C. 20545
01CY ATTN DOC CON DR. YO SONG

OTHER GOVERNMENT

INSTITUTE FOR TELECOM SCIENCES
NATIONAL TELECOMMUNICATIONS & INFO ADMIN
BOULDER, CO 80303
01CY ATTN A. JEAN (UNCLASS ONLY)
01CY ATTN W. UTLAUT
01CY ATTN D. CROMBIE
01CY ATTN L. BERRY

NATIONAL OCEANIC & ATMOSPHERIC ADMIN
ENVIRONMENTAL RESEARCH LABORATORIES
DEPARTMENT OF COMMERCE
BOULDER, CO 80302
01CY ATTN R. GRUBB
01CY ATTN AERONOMY LAB G. REID

DEPARTMENT OF DEFENSE CONTRACTORS

AEROSPACE CORPORATION
P.O. BOX 92957
LOS ANGELES, CA 90009
  01CY ATTN I. GARFUNKEL
  01CY ATTN T. SALMI
  01CY ATTN V. JOSEPHSON
  01CY ATTN S. BOWER
  01CY ATTN D. OLSEN

ANALYTICAL SYSTEMS ENGINEERING CORP
5 OLD CONCORD ROAD
BURLINGTON, MA 01803
  01CY ATTN RADIO SCIENCES

AUSTIN RESEARCH ASSOC., INC.
1901 RUTLAND DRIVE
AUSTIN, TX 78758
  01CY ATTN L. SLOAN
  01CY ATTN R. THOMPSON

BERKELEY RESEARCH ASSOCIATES, INC.
P.O. BOX 983
BERKELEY, CA 94701
  01CY ATTN J. WORKMAN
  01CY ATTN C. PRETTIE
  01CY ATTN S. BRECHT

BOEING COMPANY, THE
P.O. BOX 3707
SEATTLE, WA 98124
  01CY ATTN G. KEISTER
  01CY ATTN D. MURRAY
  01CY ATTN G. HALL
  01CY ATTN J. KENNEY

CHARLES STARK DRAPER LABORATORY, INC.
555 TECHNOLOGY SQUARE
CAMBRIDGE, MA 02139
  01CY ATTN D.B. COX
  01CY ATTN J.P. GILMORE

COMSAT LABORATORIES
LINTHICUM ROAD
CLARKSBURG, MD 20734
  01CY ATTN G. HYDE

CORNELL UNIVERSITY
DEPARTMENT OF ELECTRICAL ENGINEERING
ITHACA, NY 14850
  01CY ATTN D.T. FARLEY, JR.

ELECTROSPACE SYSTEMS, INC.
BOX 1359
RICHARDSON, TX 75080
  01CY ATTN H. LOGSTON
  01CY ATTN SECURITY (PAUL PHILLIPS)

EOS TECHNOLOGIES, INC.
606 Wilshire Blvd.
Santa Monica, Calif 90401
  01CY ATTN C.B. GABBARD
  01CY ATTN R. LELEVIER

ESL, INC.
495 JAVA DRIVE
SUNNYVALE, CA 94086
  01CY ATTN J. ROBERTS
  01CY ATTN JAMES MARSHALL

GENERAL ELECTRIC COMPANY
SPACE DIVISION
VALLEY FORGE SPACE CENTER
GODDARD BLVD KING OF PRUSSIA
P.O. BOX 8555
PHILADELPHIA, PA 19101
  01CY ATTN M.H. BORTNER
    SPACE SCI LAB

GENERAL ELECTRIC COMPANY
P.O. BOX 1122
SYRACUSE, NY 13201
  01CY ATTN F. REIBERT

GENERAL ELECTRIC TECH SERVICES
  CO., INC.
HMES
COURT STREET
SYRACUSE, NY 13201
  01CY ATTN G. MILLMAN

GEOPHYSICAL INSTITUTE
UNIVERSITY OF ALASKA
FAIRBANKS, AK 99701
  (ALL CLASS ATTN: SECURITY OFFICER)
  01CY ATTN T.N. DAVIS (UNCLASS ONLY)
  01CY ATTN TECHNICAL LIBRARY
  01CY ATTN NEAL BROWN (UNCLASS ONLY)

GTE SYLVANIA, INC.
ELECTRONICS SYSTEMS GRP-EASTERN DIV
77 A STREET
NEEDHAM, MA 02194
  01CY ATTN DICK STEINHOF

HSS, INC.
2 ALFRED CIRCLE
BEDFORD, MA 01730
  01CY ATTN DONALD HANSEN

ILLINOIS, UNIVERSITY OF
107 COBLE HALL
150 DAVENPORT HOUSE
CHAMPAIGN, IL 61820
  (ALL CORRES ATTN DAN MCCLELLAND)
  01CY ATTN K. YEH

INSTITUTE FOR DEFENSE ANALYSES
1801 NO. BEAUREGARD STREET
ALEXANDRIA, VA 22311
  01CY ATTN J.M. AEIN
  01CY ATTN ERNEST BAUER
  01CY ATTN HANS WOLFARD
  01CY ATTN JOEL BENGSTON

INTL TEL & TELEGRAPH CORPORATION
500 WASHINGTON AVENUE
NUTLEY, NJ 07110
  01CY ATTN TECHNICAL LIBRARY

JAYCOR
11011 TORREYANA ROAD
P.O. BOX 85154
SAN DIEGO, CA 92138
  01CY ATTN J.L. SPERLING

JOHNS HOPKINS UNIVERSITY
APPLIED PHYSICS LABORATORY
JOHNS HOPKINS ROAD
LAUREL, MD 20810
  01CY ATTN DOCUMENT LIBRARIAN
  01CY ATTN THOMAS POTEMRA
  01CY ATTN JOHN DASSOULAS

KAMAN SCIENCES CORP
P.O. BOX 7463
COLORADO SPRINGS, CO 80933
  01CY ATTN T. MEAGHER

KAMAN TEMPO-CENTER FOR ADVANCED
STUDIES
816 STATE STREET (P.O DRAWER QQ)
SANTA BARBARA, CA 93102
  01CY ATTN DASIAC
  01CY ATTN WARREN S. KNAPP
  01CY ATTN WILLIAM MCNAMARA
  01CY ATTN B. GAMBILL

LINKABIT CORP
10453 ROSELLE
SAN DIEGO, CA 92121
  01CY ATTN IRWIN JACOBS

LOCKHEED MISSILES & SPACE CO., INC
P.O. BOX 504
SUNNYVALE, CA 94088
  01CY ATTN DEPT 60-12
  01CY ATTN D.R. CHURCHILL

LOCKHEED MISSILES & SPACE CO., INC.
3251 HANOVER STREET
PALO ALTO, CA 94304
  01CY ATTN MARTIN WALT DEPT 52-12
  01CY ATTN W.L. IMHOF DEPT 52-12
  01CY ATTN RICHARD G. JOHNSON
        DEPT 52-12
  01CY ATTN J.B. CLADIS DEPT 52-12

MARTIN MARIETTA CORP
ORLANDO DIVISION
P.O. BOX 5837
ORLANDO, FL 32805
  01CY ATTN R. HEFFNER

M.I.T. LINCOLN LABORATORY
P.O. BOX 73
LEXINGTON, MA 02173
  01CY ATTN DAVID M. TOWLE
  01CY ATTN L. LOUGHLIN
  01CY ATTN D. CLARK

MCDONNEL DOUGLAS CORPORATION
5301 BOLSA AVENUE
HUNTINGTON BEACH, CA 92647
  01CY ATTN N. HARRIS
  01CY ATTN J. MOULE
  01CY ATTN GEORGE MROZ
  01CY ATTN W. OLSON
  01CY ATTN R.W. HALPRIN
  01CY ATTN TECHNICAL
        LIBRARY SERVICES

MISSION RESEARCH CORPORATION
735 STATE STREET
SANTA BARBARA, CA 93101
  01CY ATTN P. FISCHER
  01CY ATTN W.F. CREVIER
  01CY ATTN STEVEN L. GUTSCHE
  01CY ATTN R. BOGUSCH
  01CY ATTN R. HENDRICK
  01CY ATTN RALPH KILB
  01CY ATTN DAVE SOWLE
  01CY ATTN F. FAJEN
  01CY ATTN M. SCHEIBE
  01CY ATTN CONRAD L. LONGMIRE
  01CY ATTN B. WHITE
  01CY ATTN R. STAGAT

MISSION RESEARCH CORP.
1720 RANDOLPH ROAD, S.E.
ALBUQUERQUE, NEW MEXICO 87106
  01CY R. STELLINGWERF
  01CY M. ALME
  01CY L. WRIGHT

MITRE CORP
WESTGATE RESEARCH PARK
1820 DOLLY MADISON BLVD
MCLEAN, VA 22101
  01CY ATTN W. HALL
  01CY ATTN W. FOSTER

PACIFIC-SIERRA RESEARCH CORP
12340 SANTA MONICA BLVD.
LOS ANGELES, CA 90025
  01CY ATTN E.C. FIELD, JR.

PENNSYLVANIA STATE UNIVERSITY
IONOSPHERE RESEARCH LAB
318 ELECTRICAL ENGINEERING EAST
UNIVERSITY PARK, PA 16802
  (NO CLASS TO THIS ADDRESS)
  01CY ATTN IONOSPHERIC RESEARCH LAB

PHOTOMETRICS, INC.
4 ARROW DRIVE
WOBURN, MA 01801
  01CY ATTN IRVING L. KOFSKY

PHYSICAL DYNAMICS, INC.
P.O. BOX 3027
BELLEVUE, WA 98009
  01CY ATTN E.J. FREMOUW

PHYSICAL DYNAMICS, INC.
P.O. BOX 10367
OAKLAND, CA 94610
  ATTN A. THOMSON

R & D ASSOCIATES
P.O. BOX 9695
MARINA DEL REY, CA 90291
  01CY ATTN FORREST GILMORE
  01CY ATTN WILLIAM B. WRIGHT, JR.
  01CY ATTN WILLIAM J. KARZAS
  01CY ATTN H. ORY
  01CY ATTN C. MACDONALD

RAND CORPORATION, THE
1700 MAIN STREET
SANTA MONICA, CA 90406
  01CY ATTN CULLEN CRAIN
  01CY ATTN ED BEDROZIAN

RAYTHEON CO.
528 BOSTON POST ROAD
SUDBURY, MA 01776
  01CY ATTN BARBARA ADAMS

RIVERSIDE RESEARCH INSTITUTE
330 WEST 42nd STREET
NEW YORK, NY 10036
  01CY ATTN VINCE TRAPANI

SCIENCE APPLICATIONS, INC.
1150 PROSPECT PLAZA
LA JOLLA, CA 92037
  01CY ATTN LEWIS M. LINSON
  01CY ATTN DANIEL A. HAMLIN
  01CY ATTN E. FRIEMAN
  01CY ATTN E.A. STRAKER
  01CY ATTN CURTIS A. SMITH

SCIENCE APPLICATIONS, INC
1710 GOODRIDGE DR.
MCLEAN, VA 22102
  01CY J. COCKAYNE
  01CY E. HYMAN

SRI INTERNATIONAL
333 RAVENSWOOD AVENUE
MENLO PARK, CA 94025
  01CY ATTN J. CASPER
  01CY ATTN DONALD NEILSON
  01CY ATTN ALAN BURNS
  01CY ATTN G. SMITH
  01CY ATTN R. TSUNODA
  01CY ATTN DAVID A. JOHNSON
  01CY ATTN WALTER G. CHESNUT
  01CY ATTN CHARLES L. RINO
  01CY ATTN WALTER JAYE
  01CY ATTN J. VICKREY
  01CY ATTN RAY L. LEADABRAND
  01CY ATTN G. CARPENTER
  01CY ATTN G. PRICE
  01CY ATTN R. LIVINGSTON
  01CY ATTN V. GONZALES
  01CY ATTN D. MCDANIEL

TECHNOLOGY INTERNATIONAL CORP
75 WIGGINS AVENUE
BEDFORD, MA 01730
  01CY ATTN W.P. BOQUIST

TOYON RESEARCH CO.
P.O. Box 6890
SANTA BARBARA, CA 93111
  01CY ATTN JOHN ISE, JR.
  01CY ATTN JOEL GARBARINO

TRW DEFENSE & SPACE SYS GROUP
ONE SPACE PARK
REDONDO BEACH, CA 90278
  01CY ATTN R. K. PLEBUCH
  01CY ATTN S. ALTSCHULER
  01CY ATTN D. DEE
  01CY ATTN D/ STOCKWELL
  SNTF/1575

VISIDYNE
SOUTH BEDFORD STREET
BURLINGTON, MASS 01803
  01CY ATTN W. REIDY
  01CY ATTN J. CARPENTER
  01CY ATTN C. HUMPHREY

UNIVERSITY OF PITTSBURGH
PITTSBURGH, PA 15213
  01CY ATTN: N. ZABUSKY

DIRECTOR OF RESEARCH
U.S. NAVAL ACADEMY
ANNAPOLIS, MD 21402
  02CY

IONOSPHERIC MODELING DISTRIBUTION LIST
(UNCLASSIFIED ONLY)

PLEASE DISTRIBUTE ONE COPY TO EACH OF THE FOLLOWING PEOPLE (UNLESS OTHERWISE NOTED)

NAVAL RESEARCH LABORATORY
WASHINGTON, D.C. 20375
DR. H. GURSKY - CODE 4100
DR. P. GOODMAN - CODE 4180
DR. P. RODRIQUEZ - CODE 4706

A.F. GEOPHYSICS LABORATORY
L.G. HANSCOM FIELD
BEDFORD, MA 01731
DR. T. ELKINS
DR. W. SWIDER
MRS. R. SAGALYN
DR. J.M. FORBES
DR. T.J. KENESHEA
DR. W. BURKE
DR. H. CARLSON
DR. J. JASPERSE
Dr. F.J. RICH
DR. N. MAYNARD

BOSTON UNIVERSITY
DEPARTMENT OF ASTRONOMY
BOSTON, MA 02215
DR. J. AARONS

CORNELL UNIVERSITY
ITHACA, NY 14850
DR. W.E. SWARTZ
DR. R. SUDAN
DR. D. FARLEY
DR. M. KELLEY

HARVARD UNIVERSITY
HARVARD SQUARE
CAMBRIDGE, MA 02138
DR. M.B. McELROY
DR. R. LINDZEN

INSTITUTE FOR DEFENSE ANALYSIS
400 ARMY/NAVY DRIVE
ARLINGTON, VA 22202
DR. E. BAUER

MASSACHUSETTS INSTITUTE OF TECHNOLOGY
PLASMA FUSION CENTER
LIBRARY, NW16-262
CAMBRIDGE, MA 02139

NASA
GODDARD SPACE FLIGHT CENTER
GREENBELT, MD 20771
DR. R.F. BENSON
DR. K. MAEDA
Dr. S. CURTIS
Dr. M. DUBIN

COMMANDER
NAVAL AIR SYSTEMS COMMAND
DEPARTMENT OF THE NAVY
WASHINGTON, D.C. 20360
DR. T. CZUBA

COMMANDER
NAVAL OCEAN SYSTEMS CENTER
SAN DIEGO. CA 92152
MR. R. ROSE - CODE 5321

NOAA
DIRECTOR OF SPACE AND ENVIRONMENTAL LABORATORY
BOULDER, CO 80302
DR. A. GLENN JEAN
DR. G.W. ADAMS
DR. D.N. ANDERSON
DR. K. DAVIES
DR. R. F. DONNELLY

OFFICE OF NAVAL RESEARCH
800 NORTH QUINCY STREET
ARLINGTON, VA 22217
DR. G. JOINER

LABORATORY FOR PLASMA AND FUSION ENERGIES STUDIES
UNIVERSITY OF MARYLAND
COLLEGE PARK, MD 20742
JHAN VARYAN HELLMAN, REFERENCE LIBRARIAN

PENNSYLVANIA STATE UNIVERSITY
UNIVERSITY PARK, PA 16802
DR. J.S. NISBET
DR. P.R. ROHRBAUGH
DR. L.A. CARPENTER
DR. M. LEE
DR. R. DIVANY
DR. P. BENNETT
DR. F. KLEVANS

PRINCETON UNIVERSITY
PLASMA PHYSICS LABORATORY
PRINCETON, NJ 08540
DR. F. PERKINS

SCIENCE APPLICATIONS, INC.
1150 PROSPECT PLAZA
LA JOLLA, CA 92037
DR. D.A. HAMLIN
DR. L. LINSON
DR. E. FRIEMAN

STANFORD UNIVERSITY
STANFORD, CA 94305
DR. P.M. BANKS

U.S. ARMY ABERDEEN RESEARCH
AND DEVELOPMENT CENTER
BALLISTIC RESEARCH LABORATORY
ABERDEEN, MD
DR. J. HEIMERL

GEOPHYSICAL INSTITUTE
UNIVERSITY OF ALASKA
FAIRBANKS, AK 99701
DR. L.C. LEE

UNIVERSITY OF CALIFORNIA
LOS ALAMOS SCIENTIFIC LABORATORY
J-10, MS-664
LOS ALAMOS, NM 87545
DR. M. PONGRATZ
DR. D. SIMONS
DR. G. BARASCH
DR. L. DUNCAN
DR. P. BERNHARDT
DR. S.P. GARY

UNIVERSITY OF ILLINOIS
DEPT. OF ELECTRICAL ENGINEERING
1406 W. GREEN STREET
URBANA, IL 61801
DR. ERHAN KUDEKI

UNIVERSITY OF CALIFORNIA,
LOS ANGELES
405 HILLGARD AVENUE
LOS ANGELES, CA 90024
DR. F.V. CORONITI
DR. C. KENNEL
DR. A.Y. WONG

UNIVERSITY OF MARYLAND
COLLEGE PARK, MD 20740
DR. K. PAPADOPOULOS
DR. E. OTT

JOHNS HOPKINS UNIVERSITY
APPLIED PHYSICS LABORATORY
JOHNS HOPKINS ROAD
LAUREL, MD 20810
DR. R. GREENWALD
DR. C. MENG

UNIVERSITY OF PITTSBURGH
PITTSBURGH, PA 15213
DR. N. ZABUSKY
DR. M. BIONDI
DR. E. OVERMAN

UNIVERSITY OF TEXAS
AT DALLAS
CENTER FOR SPACE SCIENCES
P.O. BOX 688
RICHARDSON, TEXAS 75080
DR. R. HEELIS
DR. W. HANSON
DR. J.P. McCLURE

UTAH STATE UNIVERSITY
4TH AND 8TH STREETS
LOGAN, UTAH 84322
DR. R. HARRIS
DR. K. BAKER
DR. R. SCHUNK
DR. J. ST.-MAURICE

PHYSICAL RESEARCH LABORATORY
PLASMA PHYSICS PROGRAMME
AHMEDABAD 380 009
INDIA
P.J. PATHAK, LIBRARIAN

END

FILMED

1-86

DTIC